AIMS Energy, 13(2): 354–401.
DOI: 10.3934/energy.2025014
Received: 28 October 2024
Revised: 05 March 2025
Accepted: 20 March 2025
Published: 28 March 2025

http://www.aimspress.com/journal/energy

Review

Optimization research on laminated cooling structure for gas turbines: A review

Xiaojing Tian[1,2,*], Weiqi Ye[3], Liang Xu[3,*], Anjian Yang[1,2], Langming Huang[1,2] and Shenglong Jin[3]

[1] State Key Laboratory of Clean and Efficient Turbomachinery Power Equipment, Deyang 618000, China
[2] Dongfang, Electric Corporation Dongfang, Turbine Co., LTD, Deyang 618000, China
[3] School of Mechanical Engineering, Xi'an Jiaotong University, Xi'an, Shaanxi 710049, China

* **Correspondence:** Email: tianxiaojing@dongfang.com, xuliang@mail.xjtu.edu.cn; Tel: +86-18728074770, +86-02983395089.

Abstract: Against the background of increasing gas turbine inlet temperature and decreasing amount of cooling air, laminated cooling structure (LCS) is a highly efficient composite cooling structure with the advantages of lower cooling air consumption and higher cooling efficiency, which is a promising development direction for future wall cooling technology. In this review, we provide an overview of LCS's structural optimization research. The experimental and simulation studies therein were reviewed, and the major influencing parameters in the structure were analyzed in detail. The characteristics of various optimization methods were investigated, and the research methodology and optimization process of multi-objective optimization of laminated cooling structure were summarized. The review shows that laminated cooling structure, as a kind of composite cooling structure, has numerous geometrical and flow factors affecting its cooling efficiency. Multi-objective optimization techniques have effective application prospects in this field. In the future, researchers should focus on enhancing the efficiency and accuracy of multi-objective optimization algorithms. They should also explore the application of machine learning and artificial intelligence in LCS optimization, thereby promoting the intelligence and automation of design optimization.

Keywords: gas turbine; laminated cooling structure; composite cooling; multi-objective optimization; parameter analysis; optimization research

Nomenclature: LCS: laminated cooling structure; TIT: turbine inlet temperature; ML: machine learning; CFD: computational fluid dynamics; OED: orthogonal experimental design; ITI: infrared thermal imaging; TM: thermocouple measurement; TLC: thermochromic liquid crystal; HTC: heat transfer coefficient; DNS: direct numerical simulation; RANS: Reynolds averaging Navier-Stokes; LES: large eddy simulation; SST: shear stress transport; CHT: conjugate heat transfer; FE: finite element; TPMS: triply periodic minimal surface; TO: topology optimization; AM: additive manufacturing; NUD: non-uniform hole diameter; DKTS: droplet-shaped Kagome truss structure; CPF: circular pin fins; DPF: droplet-shaped pin fins; CKTS: circular Kagome truss structure; TBC: thermal barrier coating; LHS: Latin hypercube sampling; RBFNN: radial basis function neural network; NSGA-II: second-generation non-dominated sequential genetic algorithm; DL: Deep learning; ANN: artificial neural network; DQN: deep Q-network; CNN: convolutional neural network; RNN: recurrent neural network; MOP: multi-objective optimization problem; MOGA: multi-objective genetic algorithm; PSO: particle swarm optimization; GA: genetic algorithm; η_a: adiabatic film cooling efficiency; η: overall cooling efficiency; T_∞: mainstream temperature; T_c: initial coolant temperature; T_w: conjugate cooling wall temperature; η_l: line average cooling efficiency; η_S: area average cooling efficiency; C_p: total pressure loss coefficient; p_c: coolant inlet pressure; p_∞: mainstream inlet pressure; p_{out}: mainstream outlet pressure; m_c: coolant mass flow rate; m_∞: mainstream mass flow rate; ρ_∞: mainstream density; v_∞: mainstream velocity; C_f: flow coefficient; S_c: coolant outflow area; Rg: gas constant of air; γ: specific heat of the coolant; Nu: Nusselt number; Q: heat flux at the target surface; L: characteristic length; λ: thermal conductivity of the fluid; $\overline{Nu}_S$: surface-averaged Nusselt number; BR: blowing ratio; ρ_c: density of the coolant; u_c: velocity of the coolant; ρ_∞: density of the mainstream; u_∞: velocity of the mainstream; L/D: length-to-diameter ratio

1. Introduction

Heavy-duty gas turbines are hailed as the ‘pearl of the crown’ in the equipment manufacturing industry, representing the comprehensive level of development across multiple theoretical disciplines and engineering fields. They are widely used in industrial equipment such as aviation propulsion systems, marine power plants, and land-based power generation equipment [1,2]. With the continuous development of the aviation industry, countries around the world are demanding increasingly higher performance from aircraft engines. They not only seek higher thrust-to-weight ratios, greater stability, and reliability, but also aim to reduce energy consumption and minimize greenhouse gas emissions [3]. According to the Brayton cycle theory, increasing the turbine inlet temperature (TIT) results in higher cycle efficiency and power output [4]. This improvement helps the fuel burn more fully and reduces carbon emissions [5]. The TIT of high-performance aero-gas turbine engines has surpassed 2000 K [6], and it is anticipated that in the future, the temperature in afterburners will exceed 2200 K [7]. The persistent enhancement of performance technical indicators for gas turbines poses a formidable challenge to the thermal protection technologies of hot-end components (such as combustor liners, turbine blades, fuel nozzles, etc.)

To ensure safety and prolong the service life of components, the development of efficient active cooling technologies is imperative. However, the existing cooling technologies, primarily based on film cooling, encounter a prominent contradiction in terms of the volume of cooling air utilized. First, the increase in the amount of air involved in combustion leads to a reduction in the amount of air available for cooling. Second, the improvement in the compression ratio of the compressor leads to an

increase in the temperature of the cooling air, thereby diminishing the cooling potential of the air and failing to achieve the desired cooling effect. Unrestricted increases in the use of cooling air can exacerbate the mixing losses between cold and hot gases [8], leading to the quenching of combustion flames close to the wall [9]. Furthermore, to comply with environmental regulations, the emission limits for pollutants from gas turbines are continually being revised, with the specified emission values persistently decreasing [10]. This further requires more air for combustion. It is evident that the effective use of less cooling air is the trend for future high-efficiency cooling technologies.

Generally speaking, high-efficiency cooling structures have composite characteristics, and the fundamental structure consists of internal convection cooling and external film cooling, which utilizes limited cooling air to minimize the overall temperature of high-temperature components. The incorporation of multiple cooling units in composite cooling configuration increases flow complexity and necessitates consideration of the effects of coupled heat transfer. Therefore, the combination of different cooling configurations requires specific analysis. In the past decades, researchers have made great efforts to explore effective combinatorial strategies. These strategies include the utilization of jet impingement, ribbed walls, pits, and pin-fin arrays to enhance internal convection cooling [11–14], as well as the employment of shaped holes, slopes, and grooves to enhance external film cooling [15–18]. These explorations have provided technical means for the efficient utilization of cooling air for thermal protection and have established a research foundation for the integration of various cooling schemes.

The development of gas turbine blade cooling structures has evolved significantly over the years. Early cooling methods relied on simple convective cooling, where cooling air flowed through internal passages to manage blade temperatures. A few decades ago, as TIT rose, more advanced techniques such as impingement cooling combined with film cooling were introduced. These traditional cooling structures, often referred to as impingement/film or impingement/effusion cooling systems, used cooling air to impinge on the blade surface and form a protective film, enhancing local heat transfer but with limited overall effectiveness due to non-uniform cooling air distribution. Modern double-wall cooling structures represent a significant advancement, incorporating multiple cooling techniques into an integrated system. These structures feature two layers with a space in between, enabling complex cooling air pathways that include impingement cooling, pin fin cooling, and film cooling. The core difference lies in the enhanced heat transfer mechanisms enabled by the double-wall design, which significantly increases the heat transfer surface area and improves cooling air distribution. This results in a more uniform temperature distribution across the blade surface, reducing thermal stresses and enhancing overall cooling effectiveness. In contrast to traditional cooling structures, modern double-wall cooling structures provide superior thermal management capabilities, making them a crucial development in the field of gas turbine blade cooling.

Laminated cooling structure (LCS) is representative of these modern integrated cooling schemes, combining internal impingement cooling, convection cooling, and external film cooling. The laminated cooling system comprises three core components: An impingement plate, a film plate, and an intermediate support structure. The impingement plate and film plate are respectively perforated with jet holes and film holes to accommodate coolant flow. The support structure (e.g., pin fin arrays, cellular lattices, or baffle-type configurations) performs dual functions: Mechanically integrating the two plates to ensure structural integrity while enhancing thermal protection performance. This enhancement is achieved through flow disturbance effects and increased contact surface area with the coolant medium. Figure 1 presents a schematic diagram of the LCS. The fundamental construction of the laminate structure includes a double-wall panel, where the film cooling plate also serves as the

target plate for impingement cooling. The advantage of this combination is that the high cooling efficiency of the impingement jets reduces the distribution density of the film holes, decreases the aerodynamic losses caused by film discharge, and simultaneously reduces the consumption of cooling air. Additionally, when forming the film cooling, it also reduces the steep temperature gradients, which can help minimize the occurrence of cracks and deformation. Panda et al. [19] compared the flow structures of film cooling and this joint configuration. It was observed that the combined scheme showed advantages over the single film cooling scheme. The turbulent kinetic energy at the outlet of the film holes decreased by 52% compared to film cooling. Wang et al. [20] found that the combined scheme effectively reduced the localized regions of low cooling performance and enhanced the uniformity of the cooling effect compared to the single film cooling. In double-wall cooling systems, different cooling configurations make a significant difference. Li et al. [21] investigated different cooling configurations on gas turbine blades, including impingement-only, film-only, impingement-film-combined, and laminated cooling configurations. The results showed that the inclusion of impingement and pin fins in the film cooling as well as the reduction of wall thickness can significantly improve the cooling efficiency.

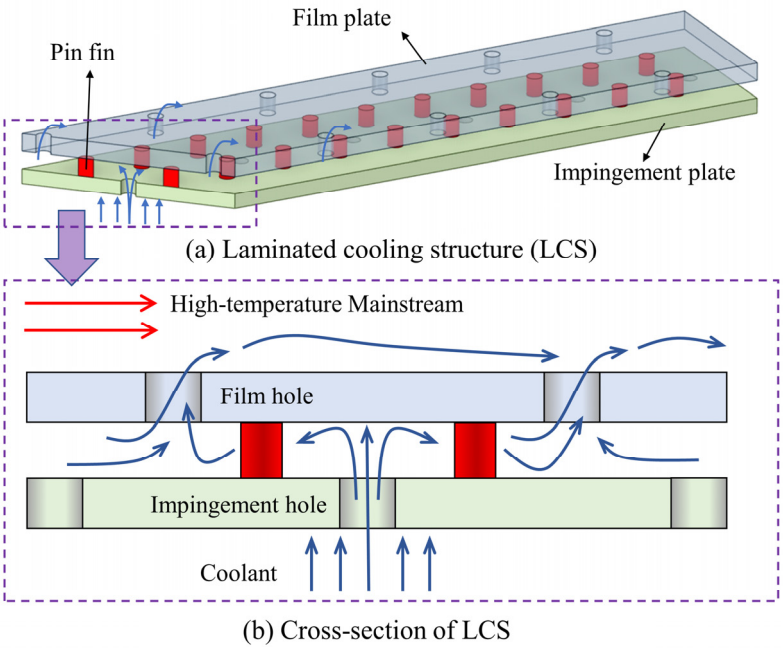

Figure 1. Schematic diagram of the laminated cooling structure.

Colladay [22] analyzed the gas turbine wall cooling scheme earlier and was the first to propose the concept of laminated cooling in 1972. He argued that the cooling gas should absorb as much heat as possible from the substrate by forced convection heat transfer before forming a protective film cooling, which reduces the flow of cooling air. A laminated cooling structure was initially used for combustion chamber cooling. Nealy and Relder [23] studied combustion chamber liners using LCS. The results showed an overall cooling efficiency of over 0.7 and a reduction in coolant usage of about 67%. This laminate configuration was successfully used in aero-engine combustion chambers at Rolls-Royce's Spey and Tay [24,25]. In the following decades, LCS was attempted for turbine blade cooling. Turbine blades with LCS were first designed by Allison, named Lamilloy, with a cooling efficiency of more

than 0.6 [26]. Laminated cooling, as an efficient cooling method with low cooling air consumption, is a promising development direction for the future cooling of gas turbines' hot-end components [27].

In comparison with film cooling structure, LCS is relatively more complex, with higher manufacturing costs and processing difficulties, and is less convenient to maintain. Therefore, the engineering application of LCS requires a high level of technical expertise. However, its ability to achieve superior cooling effects with a reduced amount of cooling gas gives it a strong competitive edge over other advanced cooling solutions. To date, General Electric (GE) of the United States has indicated that the LCS remains a promising cooling technology within the field of gas turbine heat transfer [28]. Nonetheless, if not designed properly, the LCS can be prone to certain defects: A significant temperature gradient between the cold and hot sides, substantial thermal stress, intricate manufacturing processes, high flow resistance, and increased structural weight. These issues can significantly hinder its widespread adoption and utilization. Traditional cooling structure design relies on trial-and-error optimization through experimentation and numerical simulation, focusing on single-parameter analysis and the development of correlation formulas. As a composite cooling structure, the LCS has more geometric parameters than a single cooling method, and these parameters' impact on performance indicators may not be linearly related. There may also be interactive effects between these geometric parameters and performance indicators, which complicates revealing the LCS's cooling mechanisms and leads to significant errors in formula fitting. Consequently, this challenges the traditional single-parameter model-based matching design to identify the optimal structural parameters for specific operating conditions.

Kim et al. [29] reviewed the design methodology for the development of new combustion chambers for advanced gas turbines and pointed out that the development of combustion chambers for gas turbines has entered the optimization stage, which requires consideration of the interrelationships of various technologies. Optimized design mechanisms and reasonable performance evaluation methods are very important to reduce testing and increase the effectiveness of the design. Zhang et al. [30] summarized the optimization design efforts of external film cooling and internal cooling for gas turbines. The review showed that higher single-objective or multi-objective thermal performance balanced by other constraints can be achieved by reliable and accurate optimization procedures combined with conjugate heat transfer analysis. Xu et al. [31] reviewed the application of machine learning (ML) to the optimization of gas turbines for turbine cooling, including internal cooling, external cooling, and composite cooling structures. It was pointed out that structural optimization using ML needs to be combined with multi-objective analysis where the three major factors are variable selection, objective function, and constraints.

These reviews indicate that the structural optimization of gas turbines is moving towards the formation of an integrated and automated design system. Such a system would integrate preliminary design, numerical simulation, optimization algorithms, and experimental validation into a cyclical process. Given the complexity of the interaction mechanisms among various factors in laminate structures, a multitude of research methods is required for analysis and discussion. To date, no study has conducted a systematic summary of the optimized design of the LCS. This work fills this gap. We review the optimization studies of laminated cooling structures. In chapter 2, we review previous experimental and numerical simulation studies, including performance evaluation indexes, experimental systems, simulation methods, and novel structures. In chapter 3, we analyze the optimization parameters, including film cooling parameters, internal cooling parameters, and wall factors. In chapter 4, we introduce the intelligent optimization method, and the addition of algorithmic

means such as multi-objective optimization makes the optimization of the LCS more efficient. Finally, the flow of the whole optimization process is summarized. This content can be used as a reference for optimizing the cooling of hot-end components of gas turbines in the future.

2. A review of experimental and simulation research on LCS

Although laminated cooling technology has entered the engineering application phase, researchers lack an in-depth and systematic understanding of the underlying mechanisms behind this composite cooling method. Theoretical and empirical formulas for the composite LCS design have yet been established; thus, more detailed and fundamental computational and experimental studies continue to be conducted. Previous research on the LCS has primarily focused on experimenting with and numerically simulating various structural combinations of different structures to form novel configurations, analyzing their internal flow and heat transfer mechanisms, with the aim of achieving structures that provide strong heat transfer and minimal flow resistance.

2.1. Flow and heat transfer evaluation metrics

Before reviewing LCS studies, it is necessary to understand the evaluation metrics related to flow heat transfer in gas turbine thermodynamics and computational fluid dynamics (CFD) to effectively guide structural optimization. Due to varying research objectives and structural configurations, the parameters used by researchers are not uniform. More often than not, certain dimensionless parameters are derived from previous formulas. Listing all previous evaluation metrics is impractical. Below, only a few commonly used evaluation metrics in the design of the LCS are presented.

The adiabatic film cooling efficiency (η_a) and the overall cooling efficiency (η) are important metrics for evaluating wall cooling configurations [32]. The normalized form of the adiabatic film cooling efficiency is often used for the assessment of film cooling performance, and this dimensionless cooling performance parameter is based on the assumption that there is no thermal conductivity within the solid wall surface and is defined as follows:

$$\eta_a = \frac{T_\infty - T_{aw}}{T_\infty - T_c} \tag{1}$$

where T_∞ is the mainstream temperature, T_{aw} is the adiabatic wall temperature, and T_c is the initial coolant temperature.

The overall cooling efficiency takes into account the performance of the entire cooling system and is applicable to composite cooling structures. It is a universal efficiency because it highly couples the effects produced by conjugate conduction, convection, and film coverage [33]. It is defined as follows:

$$\eta = \frac{T_\infty - T_w}{T_\infty - T_c} \tag{2}$$

where T_w is the conjugate cooling wall temperature.

The resulting average cooling efficiency of the derived lines and surfaces can be calculated by the following equation [34]:

$$\eta_l = \frac{\int (T_\infty - T_w) dl}{(T_\infty - T_c) l} \tag{3}$$

$$\eta_S = \frac{\iint (T_\infty - T_w) dS}{(T_\infty - T_c) S} \tag{4}$$

where l and S represent the selected line and area, respectively. For digitized images, they represent pixel points on lines and surfaces.

The complex internal structure of a composite LCS inevitably increases flow resistance and pressure loss while enhancing internal convective heat transfer. When evaluating a heat transfer enhancement method, especially for complex structures, the total pressure loss coefficient (C_p) is involved. The C_p reflects the flow energy loss resulting from the cooling configuration. Laminated cooling involves the mixing of the main flow stream and the coolant, which requires a weighted correction for the inlet pressure of both [35]. Referring to the definition of Zhang [36], it is calculated as follows:

$$C_p = \frac{\frac{p_c m_c}{(m_c + m_\infty)} + \frac{p_\infty m_\infty}{(m_c + m_\infty)} - p_{out}}{0.5 \rho_\infty v_\infty} \tag{5}$$

where p_c is the coolant inlet pressure, p_∞ is the mainstream inlet pressure, p_{out} is the mainstream outlet pressure, m_c is the coolant mass flow rate, m_∞ is the mainstream mass flow rate, ρ_∞ is the mainstream density, and v_∞ is the mainstream velocity.

The flow coefficient (C_f) represents the ratio of the actual flow rate to the ideal flow rate, reflecting the frictional resistance and flow losses of the structure. Referring to the definition of Bunker [37], it is calculated as:

$$C_f = \frac{m_c}{\frac{p_c S_c}{\sqrt{RgT_c}} \sqrt{\left(\frac{2\gamma}{\gamma - 1}\right)\left[\left(\frac{p_{out}}{p_c}\right)^{\frac{2}{\gamma}} - \left(\frac{p_{out}}{p_c}\right)^{\frac{\gamma+1}{\gamma}}\right]}} \tag{6}$$

where S_c is the coolant outflow area, Rg is the gas constant of air, and γ is the specific heat of the coolant.

Nusselt number (Nu) is a dimensionless number used to describe the strength of convective heat transfer. It is defined as the ratio of convective heat transfer to thermal conductivity and is given by:

$$Nu = \frac{QL}{(T_w - T_{aw})\lambda} \tag{7}$$

where Q is the heat flux at the target surface; L is the characteristic length, which in LCS is generally the diameter of the impact hole or film hole; and λ denotes the thermal conductivity of the fluid.

Considering that the pin fins expand the target plate area, the surface-averaged Nusselt number will also generally be used to synthesize the analysis, one form of which is:

$$\overline{Nu_S} = \frac{\iint Nu \, dS_{target} + \iint Nu \, dS_{pin}}{S_{target} + S_{target-pin}} \tag{8}$$

where S_{target}, S_{pin}, and $S_{target-pin}$ are the target plate area, the side area of the pin fins, and the target plate area occupied by the pin fins, respectively.

The refined design of high-temperature components not only focuses on the level of heat transfer, but also attaches great importance to the problem of heat transfer uniformity. However, there are not many evaluation metrics for heat transfer uniformity of laminated cooling, and there is not a unified

evaluation metric. Ji et al. [38] expressed the heat transfer uniformity of the heat transfer surface by using the $\overline{Nu_S}$ and the zonal-averaged Nu, and the results showed that changing the diameter of the jets in the direction of the flow direction could reduce the influence of the cross-flow on the impingement of the downstream jets. Compared with the conventional impingement cooling structure with equal diameter configuration, the configuration with the diameter of the impingement holes increasing first and then decreasing provides a higher level of heat transfer and more uniform cooling. Zhou et al. [39] defined non-uniformity coefficients to represent the heat transfer uniformity, and it was found that the distribution of jet diameters has no significant effect on the flow losses and the overall heat transfer, but the mass-velocity ratio in the impingement interval and the heat transfer uniformity are greatly affected. Yao et al. [40] considered the uniformity of cooling in the multi-objective optimization design of the laminated cooling structure, and the relative standard deviation of the outer surface temperature was used as a criterion for evaluating the temperature uniformity, and the closer the value is to 0, the more uniform the temperature is indicated. The results show that the LCS with fan-shaped film holes has the best temperature uniformity with deviations within 5%.

2.2. Experimental investigation of the LCS

Modern experimental techniques play a pivotal role in the development of LCS optimization, serving not only as a critical tool for screening initial design concepts but also as an essential source for validating data in thermal design analysis. With the development of technology, researchers in the field of heat transfer have been increasingly detailed and perfected the study of jet impingement cooling, film cooling, and composite cooling related to laminated cooling. Furthermore, heat transfer experiments need to use experimental instrumentation that is also in rapid development such as infrared thermography, temperature-sensitive paint, and liquid crystal. The experimental environment is guaranteed, the experimental means are further improved and refined, and the accuracy and credibility of the experimental results are strengthened, which makes people's research on laminated cooling technology further strengthened. Since the use of actual blades to study laminated cooling is too expensive, has poor economy, is not suitable for scientific research, and the general experimental conditions cannot really simulate the internal heat exchange of actual working blades, the existing experiments often use modeled unit test pieces. The experimental research on the LCS is mainly the influence of the change of geometrical structure parameters on its flow characteristics and wall heat transfer law and cooling effect, and a large number of research results have been obtained, which strengthens the connection between numerical theoretical analysis and basic application research.

The researchers need to measure the temperature of the channel wall of the experimental section of the composite laminate optimized member, the temperature of the airflow inlet and outlet inside the channel, the pressure along the flow, and the pressure state of the laminated structural unit carrying pressure, the incoming flow rate and turbulence, as well as the complex flow pattern of the airflow inside the experimental section. This is a multifactorial experimental problem, which generally uses orthogonal experimental design (OED) and analyzes the effects of the flow heat transfer characteristics of the test pieces based on orthogonal analysis methods. The general diagram of the LCS experimental system is given in Figure 2. The experimental system comprises an air compressor, an air receiver, check valves, a flowmeter, filters, an air heater, a test section, a data acquisition system, and various valves. The air, after being compressed and filtered by the air compressor, is directed into the air receiver to stabilize the pressure, which is then supplied to both the mainstream and cooling airflows.

During the experiment, the flow rates of the mainstream and cooling airflows are controlled by adjusting the inlet valves, while the outlet valves are used to regulate the outlet pressure of the mainstream and cooling airflows. In the test section part, part of the cooling airflow flows from the cold air area to the mainstream area through the unit piece, thus realizing the cooling of the LCS, and then together with the mainstream is discharged from the mainstream outlet through the check valve and silencer. The data acquisition system reads and stores the experimental laminate temperature values in real-time.

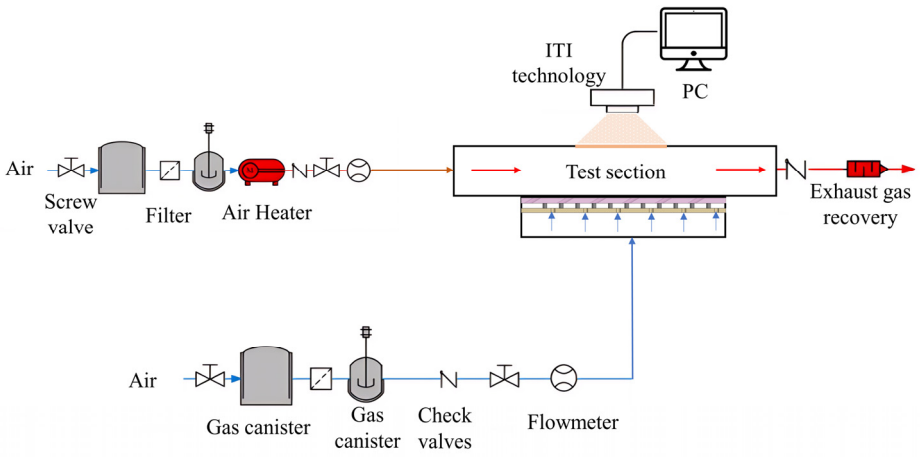

Figure 2. General diagram of the experimental system of the LCS.

A variety of experimental testing techniques have been developed by researchers in the testing segment. For the measurement of the steady-state temperature field of the laminated structure, a combination of infrared thermal imaging (ITI) techniques and thermocouple measurement (TM) is generally used due to its low uncertainty and non-contact measurement. The experiments were carried out in a high-temperature wind tunnel platform to simulate a high-temperature and high-pressure environment, and the aerodynamic performance of the structure was evaluated using a pressure transducer.

Table 1 lists the details of the LCS experimental studies. Sweeney et al. [41] used an ITI system to perform detailed two-dimensional steady-state measurements of the flat plate surface temperature of laminated cooling structure with snowflake pin fins, and investigated the effect of different temperature ratios, blowing ratios, pore spacing, and inclination of the air film pores on the cooling efficiency. Nakamata et al. [42] used an experimental approach to investigate the law of influence of the presence or absence of pin fins and the arrangement between the pore columns on the cooling efficiency, and used an infrared camera to measure the temperature distribution on the hot side of the film plate, and evaluated the area-averaged cooling efficiency versus the localized cooling efficiency of the corresponding hot side of the film plate under each model. Wang et al. [43], to validate the numerical method for a complex double-wall configuration used an infrared thermal imaging system to capture the two-dimensional temperature distribution, and used particle image velocimetry (PIV) to capture the fluid velocity distribution. The experiments were conducted in a hot gas wind tunnel with a 30-kW electric heater. Kim et al. [44] investigated experimentally the combination of impingement and evanescent cooling for a three-layer LCS and single-layer evanescent cooling in a comparative study. Infrared thermal imaging methods were used to assess the total cooling efficiency and to identify

the fully developed region of cooling performance. The results showed that the overall cooling efficiency of the LCS increased by 47% to 141% over the single plate with different blowing ratios. Wang et al. [45] conducted an ITI experimental investigation on the overall cooling performances of two turbine end-wall structures: A simple film cooling structure and a laminated structure with pin-fins and impingement holes. The study aimed to analyze and compare the cooling effectiveness of these structures under various blowing ratios and a temperature ratio close to real gas turbine operating conditions. In another study, Wang et al. [34] focused on the cooling characteristics of a vane laminated end-wall with an axial-row layout of film holes. They compared the overall cooling effectiveness and surface temperature gradients of the laminated cooling end-wall with a traditional film cooling end-wall under different mass flow ratios and temperature ratios, highlighting the benefits of the laminated structure in improving cooling performance and reducing temperature gradients. Pu et al. [46] experimentally investigated the impact of turbulence intensity on the cooling performance and thermal deformations of laminated end-walls, finding that higher turbulence intensity negatively affected cooling effectiveness. After that, Pu et al. [47] focused on the cooling air effect on the overall cooling of laminated configurations, proposing a modified design to achieve more uniform metal temperature distribution. Bai et al. [48] conducted an experimental study on the effects of geometric factors such as gap distance, impingement hole diameter, and effusion hole arrangement on the wall temperature of a novel impingement-effusion cooling system for gas turbine combustors. The researchers measured the wall temperature of the effusion plate using high-precision thermocouples and analyzed the cooling performance under various operating conditions.

Table 1. Detailed information of the LCS experimental studies.

Ref.	Year	Main research content	Material (Thermal conductivity)	Measurement technology	Re_∞	Re_c	$T_\infty(K)$	$T_c(K)$	Evaluation metric
Sweeney [41]	1999	Hole spacing and angle	6–4 Titanium	ITI	1000000~ 1800000	-	700	318~368	T_w , η
Funazaki [49]	2001	Heat transfer distribution	Acrylic-Resin	TLC, TM	-	10000	-	-	HTC
Nakamata [42]	2007	Pin / hole arrangement	Stainless Steel (17 W/(m·K)), Nickel Alloy (10 W/(m·K))	ITI	380000	5000~30000	673	290~370	η , η_S
Wang [43]	2008	Validation of numerical methods	Transparent Materia	ITI, PIV	7000	965, 1447, 1930	1023	436~455	T_w , η
Manzhao [50]	2008	Heat transfer distribution	Perspex	TLC	-	20000~50000	-	-	HTC
Wang [33]	2009	Angle of pin fins and film holes	Stainless Steel	ITI	1962	662	623	-	T_w , η , HTC
Kim [44]	2014	Comparison of two cooling methods	Transparent Material (8.9 W/(m·K))	ITI	-	-	323	304	η
Terzis [51]	2014	Different jet diameters	Acrylic Material	TLC	-	15500~52000	-	-	HTC, N_u
Zhang [52]	2016	Performance of two different film hole spacings	Plexiglas	TLC, TM	-	1000~6000	-	298~303	C_p , HTC,N_u
Wang [45]	2017	Comparison of film cooling and laminated cooling	310s Stainless Steel (18 W/(m·K))	ITI, TM	80000	-	773	313	η
Li [21]	2019	Cooling arrangement and wall thickness	Artificial Marble (1.7 W/(m·K))	ITI, TM	-	800~4500	333	293	η
Wang [34]	2019	Conjugate heat transfer effects at different temperature ratios	Titanium Alloy (7 W/(m·K))	ITI, TM	110000, 80000	-	473, 773	331~339, 380	η , η_l , η_s
Pu [46]	2020	Effects of mainstream turbulence intensity	TC4 Titanium Alloy (7 W/(m·K))	ITI, TM	110000, 80000	-	473, 773	339~341, 380~398	η , C_p
Pu [47]	2022	Improved lcs based on cooling air consumption	TC4 Titanium Alloy (7 W/(m·K))	ITI, TM	110000	-	473	315	η
Bai [48]	2023	Effects of geometric factors such as gap distance, impingement hole diameter, and effusion hole arrangement	Stainless Steel (16.3 W/(m·K))	TM	402000~ 711000	22000	-	-	η , $\bar{\eta}$

For transient temperature fields, the thermochromic liquid crystal (TLC) measurement technique can be used. The principle of operation is that the surface to be measured is coated with a layer of liquid crystal that is extremely sensitive to temperature. In the experiment, when the test piece is heated or cooled, the chromaticity of the liquid crystal changes with the temperature field. Funazaki et al. [49] proposed a narrow-band thermochromic liquid crystal technique to obtain the transient temperature field on the surface of the target plate and pin fins of a laminated structure. It was found that the jet from the shock plate induced high heat transfer on the target plate, forming a toroidal region. Manzhao et al. [50] determined the temperature and heat transfer coefficient (HTC) inside the Lamilloy configuration using the TLC transient measurement technique. The results showed that the porosity had a significant effect on the internal heat transfer of the laminate, with the larger the porosity, the higher the HTC. An approximately linear relationship between the average HTC of the internal surface and the Reynolds number was also found. Terzis et al. [51] used the transient liquid crystal technique to evaluate the heat transfer coefficient distribution inside the cooling channel. A comparison of configurations with different diameters with a uniform diameter configuration showed that different jet diameters have a significant effect on the level of heat transfer and temperature uniformity. Zhang et al. [52] carried out an experimental study of flow resistance and heat transfer coefficients for Lamilloy with two membrane pore spacings. The TLC technique was used for time mapping of surface temperature. Plexiglass with low thermal conductivity and low thermal diffusivity was used for the test section material. When the membrane pore spacing was reduced by half, the pressure loss coefficient of the membrane pore outflow increased by at least a factor of four, and the loss coefficients of the impingement jets and the channelized flow did not change much.

The experimental research on LCS has demonstrated significant advancements in enhancing the cooling effectiveness and durability of gas turbine components. However, the experimental research on LCS also faces several limitations. The complexity of manufacturing intricate internal structures, such as pin-fins and impingement holes, poses a significant challenge and increases production costs. Additionally, achieving engine-matched conditions in laboratory settings is difficult, which may limit the direct applicability of experimental results to real-world scenarios. Thermal deformation and stress analysis in LCS configurations are also complex and often not fully addressed in experimental studies, raising concerns about the long-term durability of these structures under high-temperature conditions.

Despite these limitations, the future prospects of LCS experimental research are promising. Advances in manufacturing techniques, such as additive manufacturing, can simplify the production of complex LCS structures and reduce costs. Improved experimental techniques, including high-fidelity measurements and engine-representative conditions, can provide more accurate and relevant data. Furthermore, multidisciplinary research integrating conjugate heat transfer and thermal-stress analysis can offer deeper insights into the cooling mechanisms and guide the design of more robust cooling structures. Parametric studies and adaptive cooling techniques can also lead to the development of comprehensive design guidelines and enhance the performance of LCS under various operating conditions.

2.3. Numerical investigation of the LCS

In addition to experimental methods, numerical simulation methods are also a crucial technique for studying the cooling and flow characteristics of high-temperature components of gas turbines. The advancement of computational fluid dynamics and computational heat transfer has provided a powerful tool for the numerical analysis of laminated cooling, which can meticulously study the flow field

structure within the internal channels of the laminated plate and the influence on the enhanced heat transfer, and predict the wall temperature distribution and cooling effect of the cooling structure. Part of the numerical simulation adopts the fluid-solid-thermal coupling calculation method, which directly calculates the temperature distribution of the overall calculation domain, and thus derives the cooling effect of each wall of the laminated cooling and the solid interior.

Numerical simulation is essentially based on the conservation of mass, conservation of energy and conservation of momentum, and solves the equations composed of continuity equations, conservation of energy equations, and Navier-Stokes equations [53]. Common numerical calculation methods include direct numerical simulation (DNS) [54], Reynolds averaging Navier-Stokes (RANS) [55], and large eddy simulation (LES) [56]. Among them, DNS is the most accurate simulation method, which can capture the small-scale eddy structures in the flow field in detail, but the method requires very fine and high-quality meshes, extremely high computer memory requirements, and very slow computational speeds, and is currently only applicable to simple flow heat transfer models. The LES model can utilize the filtering function to distinguish eddies according to the scale of the eddy structures, focusing only on the large-scale eddy structures that play a dominant role in the flow field, and separating the small-scale eddies from the small-scale eddy structures, and then using the filtering function to differentiate eddies. The LES model can use the filter function to differentiate the vortices according to the scale of the vortex structure, focusing only on the dominant large-scale vortex structure in the flow field, and enclosing the small-scale vortex structure with a subgrid model to speed up the calculation speed while maintaining a certain calculation accuracy [57]. However, the LES model imposes stringent requirements on the grid size and computational step size, and the extremely large number of grids and slow transient computation process make it difficult to apply this method to the study of complex 3D models. The RANS model statistically averages the control equations without the need to compute the complex turbulent instantaneous pulsations, and simply solves the time-averaged N-S equations, which greatly reduces the computational time and space, and has moderate requirements for the number and quality of grids. [58]. After comprehensive consideration of computational accuracy and computational resources, the RANS model is the most common method in turbine cooling simulation research.

The selection of turbulence models has been the focus of research in the numerical simulation of laminated cooling structures based on the RANS model. Funazaki et al. [59,60] numerically investigated the heat transfer characteristics of laminated structures with several different combinations of pin fins, and a variety of turbulence models were selected and tested, including the standard $k-\varepsilon$ model, the low-Reynolds-number $k-\varepsilon$ model, the RNG high-Reynolds-number $k-\varepsilon$, the algebraic Reynolds stress model and $k-\omega$ model. After a detailed examination of the local heat transfer coefficients, the $k-\omega$ model was chosen because it showed better predictions. The team then improved the turbulence model. The internal impingement jets were simulated using the shear stress transport (SST) $k-\omega$ model, and the external film cooling was simulated using the RNG $k-\varepsilon$ model. In fact, they pointed out in this regard that this is only a preliminary result of testing several turbulence models in CFX, and that no turbulence model can make all accurate predictions in different situations, which are related to the structure and the working conditions. Wang et al. [43] validated several turbulence models through velocimetry experiments, namely the standard $k-\omega$, SST $k-\omega$ model, RNG $k-\varepsilon$, Reynolds stress model, Realizable $k-\varepsilon$ and standard $k-\varepsilon$ model. The standard $k-\omega$ model, SST $k-\omega$ model and locally refined T-grid are recommended to study the flow field in complex channels. Panda et al. [61] performed numerical

simulations based on a double-layer air film structure with impacts using the SST $k-\omega$ model and the Realizable $k-\omega$ model, respectively, and the surface temperature of the stainless-steel plate was compared with the measured data, and it was found that the Realizable $k-\omega$ model had large simulated predictions of temperature. Gao et al. [62] numerically analyzed pin fins containing different heights, and four turbulence models were used to calculate the area-averaged cooling efficiency and the local cooling efficiency. After validation using experimental data from Nakamata et al. [63], it was found that the SST $k-\omega$ model best responded to the distribution of the local cooling efficiency. Rao et al. [64] investigated double-walled structures with pin fins and film cooling holes both experimentally and numerically simulated, and verified that the prediction of the SST $k-\omega$ turbulence model was superior to that of other turbulence models. From the above studies, it can be seen that the SST $k-\omega$ model is unanimously recognized as the best for the simulation of LCS, which is a structure with complex channels.

Laminated cooling encompasses convective heat transfer between the fluid and the solid wall, as well as heat conduction within the solid. This process involves the mutual coupling and influence of solid and fluid regions. Therefore, conjugate heat transfer analysis (CHT) computational methods are introduced to achieve a realistic comprehensive cooling efficiency. In this approach, the solid wall does not require prescribed thermal boundary conditions; the heat transfer coefficient on the wall is considered only as a process variable. Typically, the Navier-Stokes equations and energy equations are solved in the fluid region, while the heat conduction equation is solved in the solid region. Synchronization procedures are then used to link the two, facilitating the exchange of wall information. Compared to decoupled algorithms, the CHT algorithm can not only consider convective heat transfer at the fluid-solid interface and internal heat transfer within the fluid and solid regions simultaneously but also promptly update the effects of temperature field and flow field changes on material properties [65]. CHT analysis enables precise simulation of the influence of structural components, such as impingement holes and turbulator columns, on flow diversion and thermal boundary layer distribution. It elucidates the heat transfer mechanisms arising from the superposition of forced and natural convection. Furthermore, this method predicts solid thermal stresses and microstructural homogeneity, thereby providing critical foundations for optimizing cooling efficiency, reducing pressure loss, and enhancing material longevity.

In recent years, CHT analysis has been widely used. Zhou et al. [66,67] used CHT analysis to numerically study the laminated cooling models for five types of laminated cooling with different surface curvatures. The blowing ratios in a certain range were numerically investigated. Yang et al. [68] conducted experimental and CHT numerical calculations on a laminated cooling turbine end wall, and they found that the experimentally measured integrated cooling efficiency was in good agreement with the numerical calculation results, but there were some differences in the diffusion phenomena of the cold air film on the end wall surface derived from the two methods. He et al. [69] investigated the influence of gradient diameter design on cooling effectiveness and flow characteristics in double-wall cooling systems through CHT simulation, with a focus on cooling uniformity and total pressure loss under varying blowing ratios. Skamniotis et al. [70] conducted a comprehensive investigation on the influence of temperature and stress fields on the performance of double-wall cooling systems through CHT and finite element (FE) analysis, integrated with theoretical models. Their findings provided actionable optimization recommendations for enhanced design efficiency. Zhang et al. [71] established a one-dimensional CHT model through CFD simulations combined with CHT analysis. They systematically examined the influence of Reynolds number on four dimensionless parameters:

Adiabatic film cooling effectiveness, heat transfer coefficient ratio, Biot number, and temperature rise factor. A sensitivity analysis was further conducted to quantify the contributions of these parameters to the overall cooling performance. Yeranee et al. [72,73] integrated topology optimization with triply periodic minimal surfaces (TPMS) in the design of internal cooling systems. CHT simulations were employed to elucidate the flow and heat transfer characteristics as well as thermal stress distribution patterns in the novel configurations. Future CHT simulations should improve the predictability of CFD models, enhance the accuracy of turbulence modeling and improve the computational efficiency of CFD simulations for complex geometries. Table 2 lists the information from the numerical simulation studies of the LCS.

Table 2. Information on numerical simulation studies of the LCS.

Ref.	Year	Main Research Content	Analysis Tool	Grid(million)	Turbulence Model	Re_∞	Re_c	$T_\infty(K)$	$T_c(K)$
Funazaki [59]	2003	Turbulence models, pin height and pin pitch	CFX-4.4, AEA Technology	0.3	$k-\omega$	-	5000~25000	-	323
Funazaki [60]	2008	Flow behaviors and heat transfer characteristics inside and outside the integrated impingement cooling systems	ANSYS CFX-10	5.1	SST $k-\omega$	380000	4500~10600	-	-
Wang [43]	2008	The influences of inlet Reynolds numbers and the geometrical device	FLUENT 6.3	-	$k-\omega$, SST $k-\omega$	7000	965, 1447, 1930	1023	436~455
Panda [61]	2012	Conjugate heat transfer characteristics of flat plates combined with impingement and film cooling	FLUENT 13	5.8	SST $k-\omega$	-	825	318	303
Zhou [66,67]	2016	Conjugate heat transfer analysis of the effect of blowing ratio and surface curvature on overall cooling effectiveness	ANSYS CFX 14.0	5.7	SST $k-\omega$	460000	1400~10000	1600	800
Zhang [74]	2016	Cooling element layout and cooling hole injection angle	ANSYS CFX	5.5	SST $k-\omega$	49000	10000~60000	1800	800
Song [75]	2019	Cooling air flow, pressure loss and drag coefficient of six LCS	ANSYS CFX	4.5	SST $k-\omega$	-	12000	850	1900
Yang [68]	2019	Conjugate heat transfer analysis of high pressure turbine blade end walls	ANSYS CFX 15.0	16	$k-\omega$	140000~ 420000	-	298	266
Gao [62]	2021	The effect of broken pin on the flow field and cooling performance	ANSYS CFX	4.6	SST $k-\omega$	48000	10000~77000	1600	800

Continued on next page

Ref.	Year	Main Research Content	Analysis Tool	Grid(million)	Turbulence Model	Re_∞	Re_c	$T_\infty(K)$	$T_c(K)$
He [69]	2021	Conjugate heat transfer with gradient diameter film holes and impingement holes	ANSYS CFX	6	SST $k-\omega$	-	-	726	301
Skamniotis [70]	2021	Thermo-mechanical stress analysis of double wall transpiration cooling	ANSYS Fluent, ABAQUS	-	$k-\varepsilon$	-	-	1870	1000
Liu [76]	2022	Multi-parameter sensitivity analysis, influence of internal cooling structure on heat transfer characteristics	ANSYS CFX 2019 R3	24.8	SST $k-\omega$	3300	-	600	303
Song [77]	2023	Uniform hole-diameter and non-uniform hole-diameters	ANSYS Fluent	11.9	SST $k-\omega$	172000	-	297	277
Zhang [71]	2024	Cooling performance under five Reynolds numbers and three blow ratios	ANSYS CFX	5.2	Realizable $k-\varepsilon$	20000~ 400000	-	733	300
Yeranee [72,73]	2024	Conjugate simulation combined with internal cooling of TPMS	ANSYS Fluent	3.06	SST $k-\omega$	12300~ 43000	-	672	320

2.4. Novel structures in LCS

With the progressive enhancement of computer performance, the capabilities of commercial simulation software have become increasingly powerful. Numerical simulation is more convenient and faster than experimental research, and it also reduces the costs of equipment and processing [78]. Studies have indicated that the biggest challenge in fluid-solid coupling heat transfer experiments is the necessity to create an experimental environment similar to the real combustor's high-temperature and high-pressure conditions. However, generating the substantial temperature differences required for the operating environment of a combustion chamber is very expensive, and such conditions are typically not available in basic laboratories. On the other hand, when facing the optimization of small-scale structures with numerous variable parameters, it is necessary to gather a considerable amount of data as input parameters before applying optimization algorithms, which is evidently impractical through experimental methods. In recent years, thanks to the advantages of numerical simulation, researchers are no longer constrained by experimental and processing conditions, and more innovative ideas can be incorporated into the design of efficient laminated cooling structures for gas turbines.

Luo et al. [79,80] investigated the effects of pits on surface heat transfer and friction factor in double-wall and Lamilloy structures through numerical simulations, considering different pit depths, diameters, and Reynolds numbers, and gave the flow field topology following the excitation of the flow field with different pit vortex intensities. The results show that the dimple structure can induce the acceleration of the impinged fluid within the laminate inside the dimple, separation, and reattachment outside the dimple, and thus enhance the integrated heat transfer capacity inside. With the increase of pit depth, the heat transfer at the target surface initially increases and then decreases

due to the formation of large annular vortices. The increase in pit diameter first increases the heat transfer to the target surface and then decreases with the increase in flow separation. In order to reduce the flow resistance, Wang et al. [81] designed a novel cooling structure with the addition of hollow pin fins in the midst of a double wall. Figure 3 illustrates this novel structure. The hollow pin fins within the structure are connected to the impingement plate and the film plate, allowing the coolant can enter the main flow directly from the inside of the pin fins, which has a good internal cooling effect and significantly reduces the flow resistance. Moreover, the air film coverage is improved, increasing the average overall surface cooling efficiency by 14.5%. The novel cooling structure maximizes the flow coefficient by up to 32.4%, significantly reducing flow resistance.

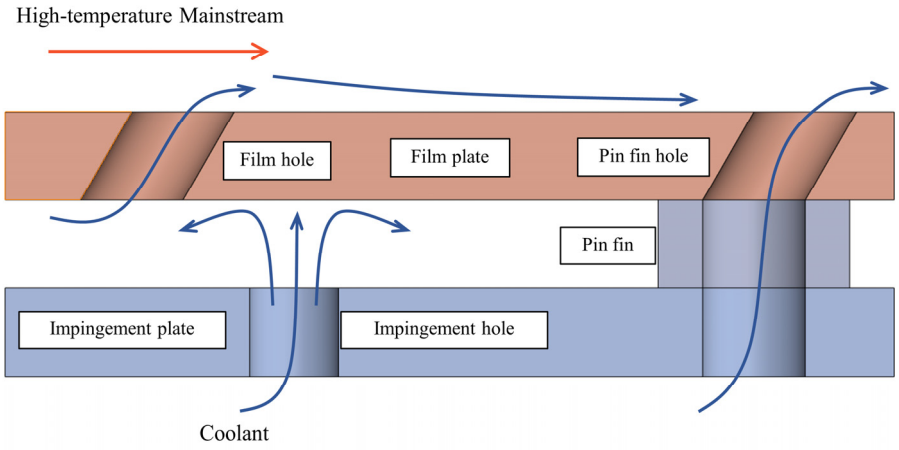

Figure 3. LCS with hollow pin fins.

Complexity of the internal structure is an optimization direction for new LCS, as convection and solid heat transfer can be enhanced. Adding partitions between each group of cooling structures to form lattice cells is a completely new idea. The cell unit formed by adding spacers has significant advantages in the laminate cooling structure, which can effectively improve the internal heat exchange efficiency and the external film cooling effect, while the pressure loss can be controlled within an acceptable range through rational design. Li et al. [82] proposed novel laminated cooling configurations with honeycomb separations and identified the heat transfer enhancement mechanisms for two new laminated cooling configurations: Honeycomb separations increase the lateral diffusion of the membrane cooling outflow and improve the external membrane cooling effect. Internal heat transfer was enhanced by the addition of membrane pore areas and partition areas in the new configuration. Chen et al. [83] developed a novel LCS with clapboards. The structure effectively improved cooling effectiveness by increasing the internal heat exchange area and intensifying the turbulence at the membrane pore outlets at high blowing ratios while controlling the total pressure loss. The new configuration achieves the highest overall cooling effectiveness, which is 9.02% to 14.08% and 2.77% to 3.54% higher than the double-wall structure and the conventional LCS, respectively. Figure 4 shows this novel clapboards configuration unit.

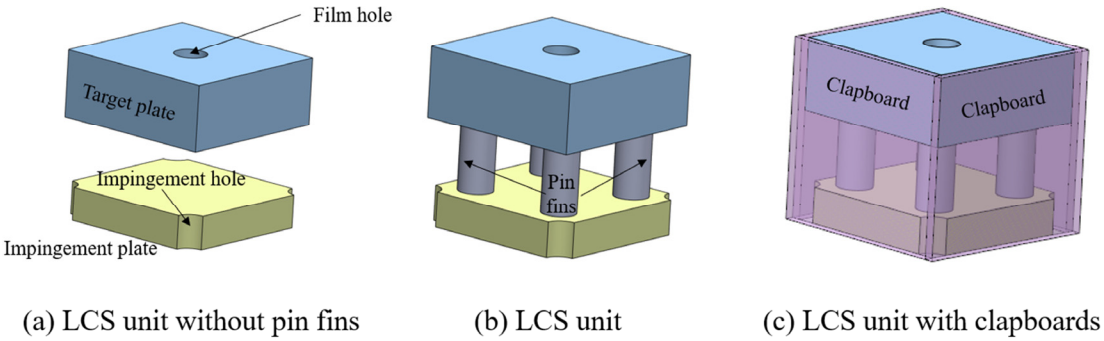

(a) LCS unit without pin fins (b) LCS unit (c) LCS unit with clapboards

Figure 4. Schematic diagram of three LCS configuration units.

Structural innovations in gas turbine laminate cooling technology, which also include cellular, bionic, and additively manufactured structures, provide new ways to improve the cooling of high-temperature components in gas turbines. Internal heat exchange efficiency can be significantly improved by topology optimization (TO) designing internal passages with specific geometries, such as TPMS structures. TO is a sophisticated structural design technique that optimizes performance by redistributing materials within a given design space. This method not only enhances design flexibility but also facilitates the creation of intricate geometries, which are especially well-suited for additive manufacturing (AM). These structures enhance convective heat exchange by increasing the internal surface area and optimizing the fluid flow path, thus improving the cooling effect. For example, TPMS structures such as Diamond, Gyroid, and I-graph show similar overall membrane cooling effects in simulations, and in some cases, these structures outperform conventional needle-like structures. Gu et al. [84] investigated a double-wall cooling system with novel slotted holes and TPMS structure and found that TPMS structure significantly improved the overall cooling efficiency while reducing the pressure loss. AM technology offers new possibilities for the design and fabrication of gas turbine laminate cooling structures. Bang et al. [85] manufactured an impingement/effusion cooling system with a hollow cylindrical structure using AM technology. This system demonstrated higher heat exchange efficiency and lower thermal stress than traditional structures. Through additive manufacturing, TPMS can also be fabricated, which is difficult to achieve by conventional manufacturing methods. The porosity and cell size of TPMS structure can be precisely controlled by AM technology to optimize the cooling effect. Yeranee et al. [72,73] filled TPMS into double-wall effusion cooling by using TO and after conjugate simulations, the results showed that the optimized model provided uniform flow inside, reduced jet lift-off, and kept the coolant attached to the effusion walls.

Similar to the role of the TPMS, in addition to filling the internal cavity of the LCS with porous media, the impingement plate and film plate on both sides can also be made of porous media to create a transpiration cooling effect. Despite the limitations of transpiration cooling in practical applications, such as low structural strength, susceptibility to particle clogging, internal oxidation, and difficulty in controlling the amount of coolant, it still shows great potential for cooling high-temperature components of gas turbines. Skamniotis et al. [70,86] investigated the application of double-wall transpiration cooling systems in gas turbine blades and hypersonic vehicles through theoretical analysis and finite element modeling, revealing critical thermal stress distributions within the dual-wall architectures. The study further explored the potential of a novel porous double-layer (PDL)

transpiration cooling technology to enhance turbine inlet temperatures, demonstrating its capacity to improve operational limits under extreme thermal conditions. Additionally, the research proposed an integrated methodology combining thermoelastic finite element analysis with Neuber-type local strain approaches to predict fatigue crack initiation, addressing critical challenges in high-cycle thermal-mechanical loading scenarios. These advancements provide a robust framework for designing cooling systems with optimized thermal efficiency and extended durability, particularly in aerospace propulsion and hypersonic thermal protection applications. In terms of heat transfer optimization, by introducing a porous layer on the surface of high-temperature components, transpiration cooling can realize efficient heat exchange and significantly reduce the surface temperature of the components. Lv et al. [87] proposed a transpiration-film combined cooling structure to enhance cooling effectiveness and reduce frictional resistance. The study demonstrates that the new structure significantly improves overall cooling effectiveness by 30% and temperature uniformity, while also reducing surface frictional resistance, making it a valuable advancement in thermal protection technology for aero-engines. In addition, transpiration cooling can also be realized by additive manufacturing technology, which is worth further research and optimization. Reseachers should continue to explore the performance of these innovative structures above in practical applications and further validate their effects through experiments and simulations. Future gas turbine cooling design needs to deeply integrate bionic principles and advanced manufacturing technologies, combined with bio-inspired smart materials (e.g., shape memory alloys, responsive hydrogels), which can develop an adaptive transpiration cooling system that dynamically adjusts the permeability according to the heat load.

3. Optimization parameters of LCS

Gas turbine blades and liners are subjected to high-temperature airflows and also experience certain mechanical vibration loads. Structural optimization needs to ensure structural strength while achieving better cooling. Conducting parametric research on LCS is essential because the influence mechanisms of these parameters are complex, and identifying the patterns of their influence helps determine the direction of optimization. Given the composite nature of the laminated structure, numerous parameters are involved. Based on the structural composition, the structural optimization of LCS is primarily divided into three aspects: Film cooling parameters, internal cooling parameters, and wall factors.

3.1. Film cooling parameters

Film cooling is a critical technology in laminated cooling systems. Figure 5 is a schematic diagram of the principle of film cooling. The secondary flow, after passing through the impingement holes and internal turbulence structures, comes into contact with the mainstream flow through the film cooling holes opened on the high-temperature wall, forming a protective layer between the wall and the mainstream, which isolates the high-temperature gas from the wall heat transfer and simultaneously absorbs some of the heat radiated to the wall. After the cooling air enters the mainstream, it undergoes entrainment and mixing, forming complex separated vortex structures, forcing the cooling air to lift [88]. This phenomenon is generally referred to as the jet separation of the cooling air and is related to the jet intensity of the cooling air and the structural parameters of the film cooling holes.

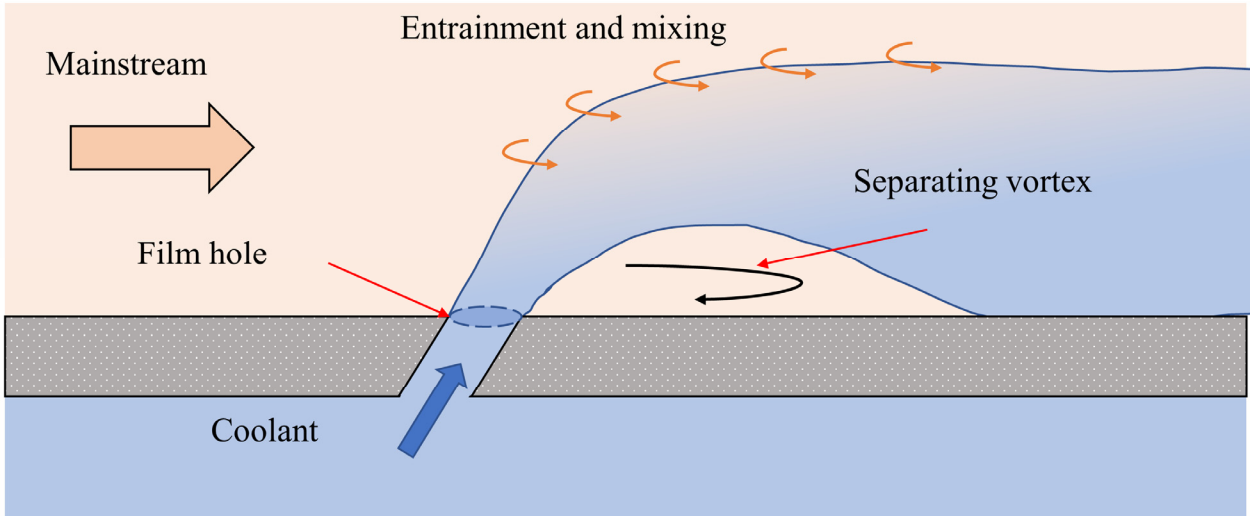

Figure 5. Schematic diagram of the principle of film cooling.

Blowing ratio (BR) is a factor affecting the intensity of the cooling air jet, defined as the ratio of the product of the density and velocity of the cooling air jet to that of the mainstream. The formula is:

$$BR = \frac{\rho_c u_c}{\rho_\infty u_\infty} \tag{9}$$

where ρ_c and u_c are the density and velocity of the coolant, and ρ_∞ and u_∞ are the density and velocity of the mainstream, respectively.

Baldauf et al. [89] experimentally measured the film cooling efficiency in the range of $BR = 0.2\sim2.5$. The results show that at low blowing ratios ($BR \leq 1.7$), the cooling efficiency increases and then decreases in the flow direction, forming a peak, while at large blowing ratios ($BR > 1.7$), the cooling efficiency increases and then stays at a constant value without a peak. Li [90,91] investigated the impact of the BR on the cooling efficiency and heat transfer coefficient of film cooling holes with different length-to-diameter ratios, noting that the cooling efficiency first increases and then decreases with the increase of the BR, while the wall heat transfer coefficient monotonically increases with the augmentation of the BR. Ignatious et al. [92] conducted numerical simulations to study the effects of the BR, hole diameter, and hole spacing on the double-wall cooling performance of combustion chamber flame tubes, pointing out that the cooling efficiency rapidly increases as the BR increases from 0.5 to 1.0, and the improvement in cooling efficiency slows down as the blowing ratio continues to increase. When the BR increases from 1.5 to 2.0, the cooling efficiency remains almost unchanged, thus considering BR of 1.5 to have the optimal cooling effect. Summarizing these studies reveals that film cooling efficiency tends to rise and then fall with the increase of the BR. The main reason for the low cooling efficiency at high BR is the jet separation phenomenon caused by the high momentum of the cooling air jet. For different film holes, the trend of film cooling efficiency variation with the blowing ratio shows certain differences. Additionally, when optimizing the film cooling hole structure, the optimal structural parameters are also influenced by the blowing ratio. Therefore, the BR is an indispensable parameter in the study of laminated cooling air.

The length-to-diameter ratio (L/D) is the ratio of the length (L) to the diameter (D) of a film hole, which often depends on the thickness of the film cooling plate, the angle of the film hole, and the

diameter of the hole itself. It is an important factor affecting the performance of film cooling. It is worth noting that due to the double-layer structure, the thickness of the film cooling plate in the LCS is significantly reduced compared to traditional film cooling structures, resulting in a substantial decrease in the L/D ratio of the film cooling holes in the LCS. A smaller L/D ratio leads to lower adiabatic film cooling efficiency and higher near-wall heat transfer coefficients. Burd et al. [93] revealed the flow mechanism of short film cooling holes and pointed out that the underdeveloped channel flow in short film cooling holes generates a strong jet penetration capability, which is an unfavorable factor affecting film coverage. Additionally, short film cooling holes can cause intense interactions between the cooling air jet and the mainstream, thereby enhancing the heat transfer near the wall. Lutum et al. [94] pointed out that within the range of $L/D < 5$, increasing L/D can significantly improve the efficiency of film cooling air. Li et al. [90] noted that the impact of L/D on cooling efficiency is limited by the blowing ratio. Under the condition of $BR < 1$, the film cooling efficiency increases with the increase of L/D; however, when $BR \geq 1$, the film cooling efficiency is the lowest at $L/D = 3.5$. In experimental studies conducted by Li et al. [95], three distinct length-to-diameter ratios (L/D) of film cooling holes (0.3, 0.35, and 0.43) were tested. When the L/D increased from 0.3 to 0.35, the average overall cooling effectiveness exhibited an improvement of approximately 2%. However, a further increase in the L/D to 0.43 resulted in a reduction of about 1% in the average overall cooling effectiveness. Zhou et al. [96] concluded that the overall cooling effect usually increases with decreasing L/D. This is because a smaller L/D implies a smaller spacing between the film holes, which improves the covering effect of the air film and enhances the cooling effect. However, when L/D is very small, it may lead to severe blockage of the first few film holes at low cooling mass flux, thus reducing the cooling effect. In summary, these results underscore the existence of an optimal L/D for film cooling holes in the design of LCS systems, which maximizes cooling performance while balancing structural and flow-dynamic constraints.

For film cooling hole arrays, non-uniform hole diameters have shown potential to improve cooling performance and reduce the risk of thermal damage in laminated cooling configurations. Song et al. [77] found that compared to traditional uniform hole diameter designs, the non-uniform hole diameter (NUD) design enhances the film effectiveness and coverage by reducing the momentum of the coolant, resulting in a relative increase of 58.7% in cooling efficiency. Moreover, it significantly reduces the near-wall instability level by eliminating separated vortex flows on the target surface, thereby reducing the risk of thermal damage. He et al. [69] demonstrated that a laminated cooling model with gradient hole diameters can improve overall cooling performance at low blowing ratios, and by optimizing the hole diameter distribution, it is possible to improve the distribution and uniformity of cooling air coverage without significantly increasing total pressure loss. These research findings indicate that NUD design provides an effective strategy for enhancing the efficiency and uniformity of laminated cooling, contributing to the enhanced thermal protection of high-temperature components such as turbine blades. The NUD design offers new insights into the cooling of actual turbine blades, especially when higher cooling efficiency is required in specific areas.

Table 3. The information on the research of film hole configuration in LCS.

Ref.	Year	Film hole configuration	Parameter range	*BR*	Method	Significant findings
Li [95]	2014	Effusion hole diameter-to-length ratio (*D/L*)	*D/L:* 0.3, 0.35, 0.43	-	EXP	As the diameter of the cooling holes increases, the flow coefficient also increases. However, the cooling efficiency is maximized when the *D/L* is 0.35.
Deng [67]	2016	Different streamwise incline angles	Incline angles: 15°, 30°,60°, 90°	0.182~1.43	NUM	A smaller inclination of the air film holes (e.g. 15°) significantly improves the cooling effect at high blowing ratios, but at the same time increases the pressure loss.
Zhang [74]	2016	Two laminated layouts with staggered arrangement，angles of film hole in streamwise direction and spanwise direction	Angles of streamwise direction and spanwise direction: 60°, 67°, 90°	0.5, 1.0, 1.5	NUM	The utilization of novel configurations and inclined film holes has enhanced the area-averaged overall cooling effectiveness by 5% to 16.2% compared to conventional designs, while simultaneously achieving a marked reduction in coolant flow resistance.
Zhou [96]	2017	Film hole length-to-diameter ratio (*L/D*)	*L/D:* 3, 4, 5, 6	0.18~1.6	NUM	The overall cooling effect usually increases with decreasing *L/D*. When *L/D* is very small, it may lead to severe blockage of the first few film holes at low cooling mass flux, thus reducing the cooling effect.
Song [75]	2019	Six LCS models: A1, A2, B1, B2, C1, C2	A1, A2: Symmetry and asymmetry; B1, B2: Cylindrical and Sectoral; C1, C2: diameter 1d and 2d	-	NUM	The shape and density of the film holes are the key factors affecting flow and drag. Fan shaped holes, while exhibiting higher flow rates at high pressure ratios, increase the drag coefficient.
Liu [97]	2020	Linear arrangement, 35°arrangement, hexagonal arrangement	Biot number: 0.17, 0.56, 2.78	0.5, 1.0, 1.5	NUM	The hexagonal arrangement of the film holes offers significant advantages in terms of improved cooling, especially at high Biot numbers and low *BR*.
He [69]	2021	Uniform diameter configuration and gradient diameter configuration	Diameter gradient: ±10%	0.5, 1, 1.5, 2	NUM	The film hole configuration with a -10% gradient exhibits optimal cooling effectiveness and uniformity under low blowing ratios, while the +10% gradient configuration demonstrates superior performance at high blowing ratios.
Song [77]	2023	Uniform diameter (UD) and non-uniform diameter (NUD)	Film hole diameter: UD: 0.4 mm; NUD: 0.4~0.55 mm	UD: 1.37~2.55. NUD: 0.65~1.74	EXP+ NUM	The NUD design significantly improves film cooling effectiveness and uniformity, especially at high flow rates.
Bai [48]	2023	Conventional arrangement, 90° rotation in the streamwise direction, 100% stretching in the streamwise direction	Pitch of film holes: 6, 7.4, 15.1 mm	0.5, 0.8, 1.5	EXP	Hexagonal arrangement and smaller gap distance show better cooling at high blowing ratios.

NUM: Numerical simulation; EXP: Experimental investigation.

The arrangement of film holes (including the inclination angle, arrangement pattern, and density of film holes) has a significant impact on the cooling performance. A shallower inclination angle of film holes (e.g., 15°) can significantly enhance the cooling effect at a high blowing ratio, but it will increase the pressure loss. The research by Deng et al. [67] indicates that for flat plates and concave surfaces, a 15° inclination angle improves the cooling effect by over 10% compared to a 90° inclination angle, while the pressure loss increases by 2.3%. The study by Liu et al. [97] reveals that the hexagonal-arranged film holes exhibit better cooling performance in the double-wall cooling system, especially at a high Biot number. The hexagonal-arranged film holes improve the cooling effect by 24.5% compared to the traditional linear arrangement. According to the research by Bai et al. [48], a dense and uniform arrangement of film holes has a very beneficial impact on improving the quality of the cooling film and the cooling performance. The cooling efficiency of the densely arranged film holes in the spanwise direction reaches 74% when the blowing ratio is 0.87.

In addition, when designing the density of film holes, it is necessary to balance the cooling effect and the pressure loss. The research by Zhang et al. [74] shows that a higher density of film holes can significantly improve the overall cooling effect, but the pressure loss also increases accordingly. Song et al. [75] suggest that when designing the LCS, both a smaller impingement hole area and a higher density of film holes should be considered to achieve the maximum inlet velocity with the minimum pressure loss. Table 3 lists the details of the research on the configuration of the film holes in the LCS. Future research should further explore the optimization schemes of film-hole arrangement under different operating conditions to improve the cooling performance and thermal efficiency of gas turbine blades.

3.2. Internal cooling parameters

Due to the integrated nature of LCS, including film cooling, impingement cooling, and internal turbulence, a multitude of structural parameters can influence the overall cooling efficiency. Li et al. [98] proposed a decoupling method for the composite construction of laminated cooling, which enables the analysis of the coupled characteristics of internal and external cooling. An important conclusion was drawn: In laminated cooling, internal cooling (mainly referring to impingement cooling and heat transfer of pin fins) contributes to most of the cooling effectiveness and heat transfer capability, while external film cooling primarily affects the distribution characteristics due to its intensive zone cooling capability. Zhang et al. [71] conducted a comprehensive study on the effects of film hole geometry on cooling performance and concluded that while the shape of film holes does influence the cooling effectiveness, the internal cooling mechanisms, such as impingement cooling and pin fin heat transfer, are the primary contributors to the overall cooling efficiency. Additionally, Gao et al. [62] investigated the impact of broken pins on cooling performance and found that the internal structure parameters have a more significant effect on the overall cooling efficiency compared to the film hole geometry. Therefore, internal cooling dominates the comprehensive cooling effect of laminated cooling, and targeted efforts to improve internal cooling performance are recommended.

The mechanism of internal cooling is based on achieving dual cooling. Within the internal structure of the LCS, the cooling air first passes through the jet holes on the cold air side wall, impacting the hot gas side wall at high-speed perpendicular to the wall to achieve the first round of cooling. When the gas impacts the target plate, the momentum of the jet is much stronger than the momentum of the surrounding fluid, causing the surrounding gas to be entrained by the high-speed

cooling jet, resulting in intense disturbance and enhanced turbulence mixing, thereby greatly improving the heat transfer capability of the impingement jet [99]. In contrast to film cooling, the cooling air in the impingement cooling process does not mix with the main combustion gas within the combustion chamber, thus not affecting the normal combustion process. Impingement cooling can achieve extremely high local heat transfer coefficients in a small area, with high cooling efficiency. However, if the diameter of the impingement hole is relatively large, it will destroy the original integrity of the structure and weaken the structural strength. After the jet impacts the film plate, it spreads outward and exchanges heat convectively with the surrounding turbulators. In this process, the remaining cooling air is fully utilized to achieve the second round of cooling.

In a laminated cooling configuration, the role of the impingement holes is to spray coolant directly onto the target surface, where the cooling effect is achieved by impingement and subsequent redistribution of cold air. Wang et al. [100] conducted numerical simulation research on the parameters of impingement holes, investigating the impingement hole diameter and impact distance. As the diameter of the impingement hole increases, the momentum of the coolant jet decreases, leading to a deterioration of the impingement cooling effect. This is due to the fact that a larger hole diameter leads to a lower jet flow rate, which reduces the ability to penetrate the main flow stream, thus weakening the momentum exchange between the coolant and the target surface. Increasing the impact distance results in an increase in momentum loss as the jet mixes with the surrounding gas, which reduces the ability for impingement cooling. Also, increasing the impact distance increases the surface area of the pin fins, which helps to increase the convective heat transfer between the coolant and the pin fins. Overall, however, an increase in impact distance usually leads to a decrease in cooling effectiveness. Wang et al. [101] investigated the geometrical parameters of the LCS, including the diameter of film holes, the diameter of impingement holes, the spreading direction and the flow spacing, by numerical simulation. The range of variation of each parameter was first investigated individually, and then the effects of these parameters on the thermodynamic performance of the laminated cooling structure were assessed by orthogonal analysis. The results are as follows: An increase in the diameter of the air film holes is conducive to improving the overall cooling effect and reducing the relative pressure drop of the cooling air; an increase in the diameter of the impingement cooling holes reduces the overall cooling effect; and a decrease in the hole spacing improves the cooling effect and the uniformity of the temperature distribution, and reduces the thermal stresses and thermal deformation.

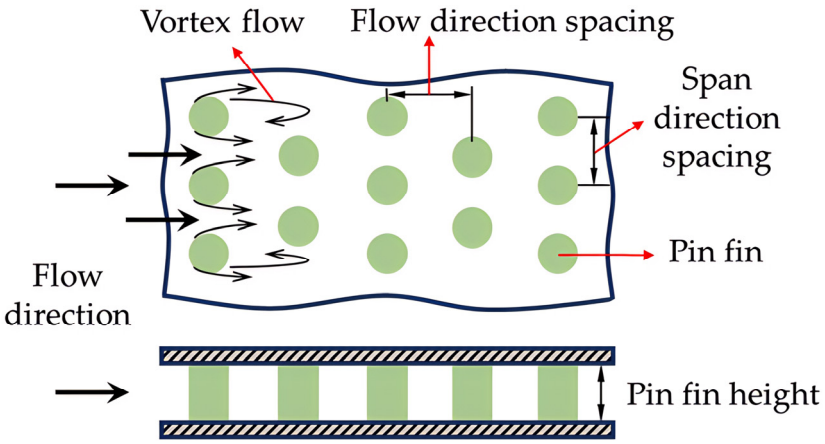

Figure 6. Structure of typical pin fins.

Due to the common practice of incorporating various forms of pin fins in laminated cooling systems, these pin fins not only enhance the disturbance effect of airflow within the channels of the cooling plate but also obstruct the airflow to achieve the injection of cooling air. Consequently, the pin fins embedded within the structure of the LCS have a significant influence on the laminated cooling performance and are a key focus in the study of laminated cooling. Numerous factors influence the heat transfer characteristics of pin fins, such as the arrangement of the pin fins, the length-to-diameter ratio, the shape of pin fins, and their position. Figure 6 illustrates the structure of typical pin fins.

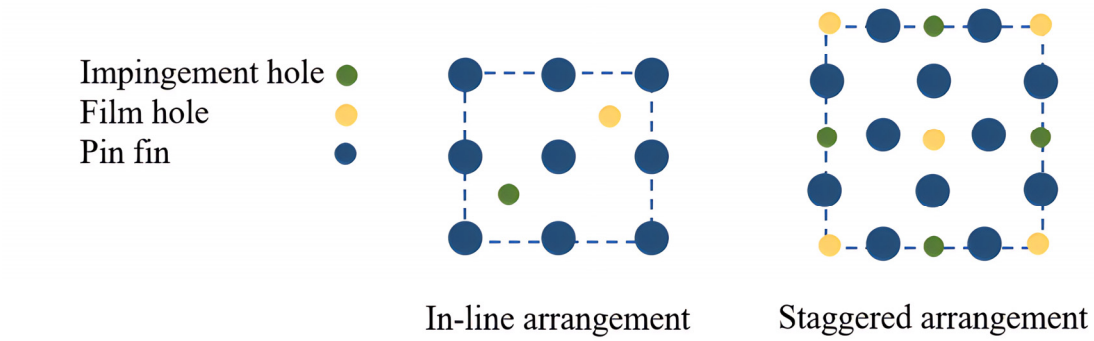

Figure 7. Two arrangements of cooling elements.

Figure 7 illustrates two different arrangements of cooling elements. The staggered arrangement of pin fins demonstrates superior performance. Xu et al. [102] experimentally studied the flow characteristics of microchannels with in-line and staggered arrangement pin fins, and analyzed for the first time the influence of pin fins arrangement on the flow transition. The flow transition was identified as a sudden increasing slope in both pressure drop versus mass flow rate curve and friction factor versus Reynolds number curve for in-line arrangement pin fins microchannel. However, no flow transition was observed in the staggered pin fins microchannel. Bianchini et al. [103] proposed a novel pentagonal arrangement in order to investigate the effect of the structural arrangement of circular pin fins arrays and compared it with a staggered arrangement. They discovered that: the pentagonal arrangement shows a non-uniform distribution of the cooling effect, with localized enhancement and attenuation at specific radial locations. Abuşka and Çorumlu [104] studied the typical sequential arrangement and staggered arrangement, and developed a new type of pin fins arrangement by changing the staggered pin fin position. The experimental results indicate that the use of an improved staggered cone pin fins arrangement design is an energy-saving option with good pressure loss, weight, and manufacturing cost values.

Furthermore, several scholars have conducted research on the arrangement density of pin fins on this basis. Nakamata [42] investigated the impact of the arrangement position of pin fins and impingement holes on the heat transfer characteristics of the LCS through experiments and numerical simulations. The results revealed that after the cold air strikes the film plate, a high heat transfer area is formed on the surface of the pin fins. The density and arrangement position of the pin fins are important parameters affecting the cooling characteristics of the LCS. The presence of pin fins makes the heat transfer characteristics of the LCS much higher than those of the impingement-film composite cooling structure, and it is not closely related to the position of the impingement holes. Bahiraei [105]

proposed a novel pentagonal arrangement in order to investigate the effect of the structural arrangement of circular pin fins arrays and compared it with a cross-arranged arrangement. They discovered that: the pentagonal arrangement shows a non-uniform distribution of the cooling effect, with localized enhancement and attenuation at specific radial locations. Ostanek [106], in order to explore whether non-uniform spacing in the flow direction could enhance heat transfer, designed a non-uniformly spaced pin fins array and compared it with a uniformly spaced pin fins array. The results show that: when the Reynolds number is low, the performance of the non-uniform array is lower than the same uniform spacing array, and maintaining a close flow field spacing between the first few rows is the key to causing turbulent mixing in the inner row. At a high Reynolds number, because the flow direction covered by the non-uniform array is 16.8% more than the uniform spacing array group, it is considered that it can bring high cooling to a larger area.

Research on the shapes of pin fins began in the early 1980s, with the initial studies focusing on cylindrical shapes [107,108]. As researchers continued to investigate the cooling mechanisms of pin fins, the cross-sectional shapes of pin fins evolved from the original circular shape to a variety of forms. Common pin fin shapes include elliptical, square, triangular, and teardrop, as well as some with irregular cross-sections, such as quincunx-shaped, star-shaped, and twisted pin fins. Zhang [109] studied the impact of different pin fin shapes on flow and cooling characteristics in three-layer LCS. Figure 8 illustrates their structures. A comparison of cylindrical, truncated conical, square, and hexagonal pin fins revealed that square pin fins have superior heat transfer coefficients and cooling efficiency in the three-layer porous laminate plate, suggesting their use as a replacement for traditional cylindrical pin fins in the combustion chamber liner cooling.

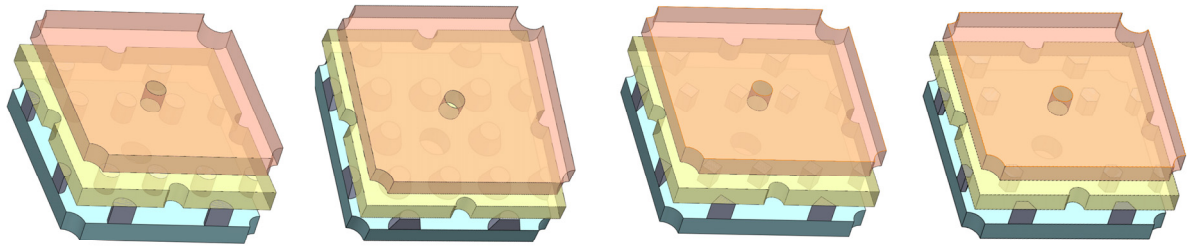

(a) Cylindrical pin fins (b) Truncated cone pin fins (c) Square pin fins (d)Hexagonal pin fins

Figure 8. Three-layer LCS with differently shaped pin fins.

Luo [110] designed a novel curved pin fin to enhance the cooling performance of LCS. The variables studied included four different inclination angles (90°, 75°, 60°, 45°) and four different lengths of vertical segments (9, 7, 5, 3 mm). Numerical calculations revealed that the curved pin fins with smaller bend angles and shorter vertical segments exhibited lower friction factors and superior thermal performance. Compared to the upright pin fins, the thermal performance of the curved pin fins with an inclination angle of 45° and a vertical segment length of 3 mm was improved by 6.1% and 14.4%, respectively. Zeng et al. [111] proposed a unique open-loop pin fin. Within each open pin fin unit, there is an internal cavity and two inner minor rings and outer major rings, with two large orifices and two minor orifices that are positioned along the streamline direction within the inner minor ring and outer major ring, respectively. The results prove that this structure can cause periodic flow separation and convergence, resulting in continuous flow mixing, periodic interruption, and re-development of the

boundary layer. Ruan [112] proposed a novel droplet-shaped Kagome truss structure (DKTS) pin fin and applied it to the jet impingement compound cooling of the intermediate chord area of gas turbine blades. Using numerical methods, DKTS was compared with circular pin fins (CPF), droplet-shaped pin fins (DPF), and circular Kagome truss structure (CKTS) in terms of flow and heat transfer. Figure 9 shows these several irregular pin fin structures. Numerical simulation results indicated that within the same porosity and jet Reynolds number range, DKTS improved the thermofluid performance by 11.1% to 17.5% compared to CKTS. DKTS and DPF compared to CPF and CKTS can reduce flow resistance and enhance heat transfer capabilities. Table 4 collects information on the parametric study of the internal cooling configuration of the LCS.

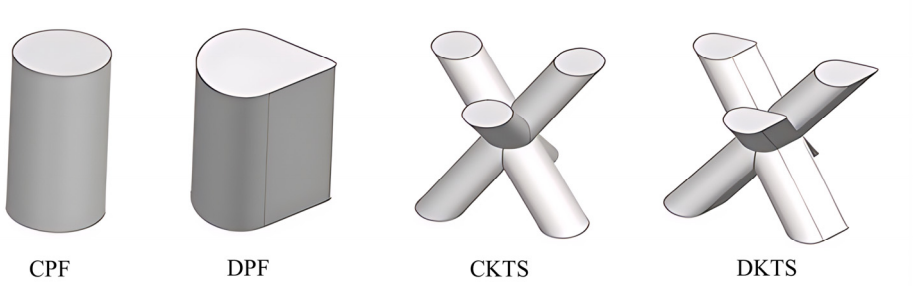

Figure 9. Special-shaped pin fins and Kagome truss structure.

Table 4. Information on the parametric study of the LCS internal cooling configuration.

Ref.	Year	Internal cooling configuration	Parameter range	Method	Significant findings
Nakamata [42]	2007	An integrated impingement and pin-fin cooling configuration	Pin fin diameter: 2.5 mm, 4.5 mm	NUM	The presence of pin fins significantly improved the local cooling effect, especially on the upstream side of the pin fins. The effect of pin fins is more obvious under the condition of high blow ratio.
Bianchini [103]	2010	An innovative pentagonal arrangement of pin fins.	Staggered arrangement and pentagonal arrangement pin fins arrays	NUM+EXP	The pentagonal arrangement shows a non-uniform distribution of the cooling effect, with localized enhancement and attenuation at specific radial locations.
Ostanek [106]	2013	A non-uniformly spaced pin fins array	Uniform spacing: 2.16, 2.60, 3.03; Non-uniform spacing: 1.73~3.46	EXP	In high Reynolds number applications, non-uniformly spaced arrays are a viable alternative that provides better heat transfer coverage. In low Reynolds number applications, uniformly spaced arrays should be preferred.

Continued on next page

Ref.	Year	Internal cooling Configuration	Parameter Range	Method	Significant findings
Xu [102]	2017	Different pin-fin arranged microchannels	In-line and staggered arrangement	EXP	In high Reynolds number applications, staggered pin-fin microchannels may be more suitable to avoid excessive pressure drops due to flow transitions.
Wang [100]	2021	Pin fin diameter (*Dp*), impingement hole diameter (*Di*), impingement height (*H*), and spanwise hole pitch (*S*)	*Dp*: 0~0.8 mm; *Di*: 0.5~1 mm; *H*: 1~3 mm; *S*: 6.8~12 mm	EXP + NUM	Increasing the diameter of the pin fin significantly improves the cooling efficiency, while increasing the diameter of the impact holes and the impact height decreases the cooling efficiency. Optimizing the hole spacing can further improve the cooling efficiency.
Zhang [109]	2021	A new three-layer porous laminate	Pin fin shapes: cylindrical, conical, square and hexagonal	EXP	The performance evaluation criteria of square pin-fin was superior to other forms.
Zeng [111]	2021	Unique type of open-ring pin fin microchannel (ORPFM)	Staggered and inline ORPFM	EXP + NUM	Thermal enhancement was achieved for ORPFM compared to rectangular microchannels. Thermal enhancement was achieved for ORPFM compared to rectangular microchannels.
Luo [110]	2022	A novel curved pin fin	Inclination angle: 90°, 75°, 60°, 45°; Vertical segment length: 9, 7, 5, 3 mm	NUM	The curved pin fins with smaller bend angles and shorter vertical segments exhibited lower friction factors and superior thermal performance.
Abuşka and Çorumlu [104]	2023	Modified staggered conical pin fin heat sink	Typical sequential, staggered and modified staggered arrangement	EXP + NUM	The use of an improved staggered cone pin fins arrangement design is an energy-saving option with good pressure loss, weight and manufacturing cost values.
Ruan [112]	2023	Droplet-shaped Kagome truss structure filled into LCS	CPF, DPF, CKTS, DKTS	EXP + NUM	Turbulators with droplet-shaped cross section have better cooling performance and lower pressure drop.

NUM: Numerical simulation; EXP: Experimental investigation.

3.3. Wall factors

In the optimization of laminated cooling structures, the wall factor is an important consideration as it directly affects the cooling efficiency and the process of heat exchange. The wall factors encompass the material of the wall, thermal conductivity, and thermal barrier coating.

The selection of materials to be used in the LCS is an important part of the optimization process, as this is a key area for improving heat transfer and heat dissipation. The selection of materials to be used in the LCS is an important part of the optimization process, as this is a key area for improving heat

transfer and heat dissipation. The base material for the gas turbines liner needs to be a high-temperature material with excellent resistance to high temperatures, oxidation, strength, and thermal and cold fatigue. Traditionally, nickel- and cobalt-based high-temperature alloys have been used for the liner, but as the gas temperature increases, the limits of the high-temperature alloys have been approached more and more.

The optimization of laminate materials can consider the use of advanced composite materials. Compared with traditional metal materials, continuous fiber toughened ceramic matrix composite (CMC) is a kind of material with low density, high specific strength, good thermo-mechanical properties, and thermal shock and impact resistance, and also has excellent oxidation and ablation resistance. CMC toughens the ceramic matrix through continuous ceramic fibers, and in the process of crack propagation, through interface separation, fiber fracture, and fiber pullout mechanisms to hinder crack extension, thus overcoming the intrinsic brittleness of ceramic materials [113]. Compared with high-temperature alloys, CMC can increase the operating temperature by more than 200°C, reduce the weight by 2/3, drastically reduce the amount of cooling gas, improve engine efficiency, and reduce greenhouse gas emissions, making them ideal materials for advanced commercial gas turbines that are more fuel-efficient and environmentally friendly [114]. It should be noted that although CMC shows great potential in gas turbine applications, there are still some challenges. Due to the unique thermophysical properties of CMC, the effectiveness of traditional impact strengthening cooling schemes may be limited. Moreover, current processing technology limitations pose challenges for implementing double-wall cooling structures using CMC materials in the near future, which calls for further research and technological breakthroughs in this area.

Optimization research of wall materials usually involves thermal conductivity. Unlike metallic materials, the thermal conductivity of composite materials is significantly anisotropic, related to many factors such as internal fibers and matrix, and not easy to measure. Low thermal conductivity in the pore areas in the matrix can cause localized heat accumulation within the wall, generating extremely high-temperature gradients, which seriously affects the service life of the component [115]. All of these bring big difficulties to the application of composites in gas turbines. Research is, on the one hand, used to simulate the thermal conductivity of composites by simplifying the crystal spores and establishing the physical calculation model of crystal spores, and to analyzing the distribution law of internal thermal stresses; on the other hand, it is used to establish the criterion relation equation to predict the thermal conductivity of composites by experiments, so as to provide relevant data support for the heat transfer of composites. The experiments of the laminate structure are conducted based on metal plates, and it is very necessary to investigate the LCS of composites, which is a direction of optimization. For laminated cooling of composites, both the heat transfer characteristics and the flow characteristics will show different characteristics from the flat plate of metallic materials.

Thermal barrier coating (TBC) technology can be used in conjunction with laminated cooling to enhance the thermal protection of hot-end components. TBC is based on the principle of covering a metal surface with a ceramic layer of very low thermal conductivity, which effectively isolates the metal wall from the high-temperature gas. Existing studies have focused on the effect of coupling passive TBC thermal protection with active cooling techniques. Mensch et al. [116] evaluated the effect of TBC on the cooling performance on the end wall of a gas turbines blade. Experimental and computational results showed that TBC significantly reduced the scaled wall temperatures in all cases. The enhancement of the cooling effect by TBC was superior to the enhancement of the cooling effect by increasing the amount of cooling air. Pu et al. [117] obtained similar conclusions from their study

of TBC on a double-walled structure. The addition of TBC on a double-walled cooling structure significantly improves the overall cooling effect of the metal, with the improvement being at least 1.7 times higher compared to increasing the cooling airflow only. Thicker TBC can attenuate the sensitivity to the blowing air ratio, thus helping to reduce the cooling air consumption. Huang et al. [118] investigated the effects of internal layout and coating thickness on the overall cooling performance of LCS when combined with TBC. The results show that the TBC provides effective protection for the LCS, and the overall cooling effect is improved by more than 20% compared with the case without TBC. The cooling effect increases with the amount of cooling air for different TBC thicknesses and internal layouts, but the addition of TBC reduces the sensitivity of the amount of cooling air to the cooling performance. To summarize the above study, the combination of TBC and laminated cooling can achieve a better cooling effect and help reduce coolant consumption, which is consistent with the purpose of LCS optimization.

From the results of the above research, it can be seen that there are many factors affecting the laminated cooling structure, and in the study of the cooling effect of the laminated structure, these factors have a promotional or restrictive relationship with each other. A LCS to obtain a better cooling effect requires a systematic study of these factors, a single parameter change cannot achieve the results we need. Therefore, in the case of practical application, the parameters of the LCS should be flexibly selected and deployed in order to match the design performance of the whole gas turbine.

4. Intelligent optimization design of LCS

The optimized design of laminated cooling structures is essential for enhancing cooling efficiency and performance. The optimization design requires repeated adjustments to both the cold air quantity and temperature distribution, which entails a variety of optimization parameters. Research and analysis based solely on a single parameter are insufficient to reveal the effects of the research parameters on the overall structure, nor can they reflect the interactive effects of the parameters on the cooling of the laminated structure. Furthermore, there are mutual constraints among the optimization objectives. Consequently, it is imperative to imperative a predictive platform utilizing intelligent optimization algorithms to facilitate multi-objective collaborative design to achieve the optimal structure.

4.1. Surrogate model

In the process of LCS intelligent optimization design, constructing a surrogate model is first required to replace time-consuming numerical simulations or experimental measurements. By leveraging historical data to fit the nonlinear mapping relationships between design parameters and optimization variables, it becomes feasible to rapidly evaluate optimization objectives in new tasks. Furthermore, by integrating the established surrogate model with appropriate optimization algorithms, optimal design configurations can be efficiently identified within the parameter space.

Common surrogate models include response surface models [119], Kriging models [120], and neural networks [121]. In recent years, these methods have been widely used in the field of intelligent optimization design of LCS. The optimization process using the surrogate model is shown in Figure 10. Lv et al. [87] took the aperture, the stream-wise spacing of holes, the span-wise spacing of holes, and the thickness of the perforated plate as design parameters, and the overall cooling effectiveness η as the optimization objective. They randomly generated 63 design points in the design space using the

Latin hypercube sampling (LHS) method and conducted CFD simulations to provide data for the training of the surrogate model. The difference between the results predicted by the Kriging surrogate model and the CFD results was less than 5%, indicating that the Kriging surrogate model can accurately predict the CFD simulation results of the LCS structure. Liu et al. [122] took the slot height S, the stream-wise inclination angle α, the diameter of the impingement hole, and the pin-fin filling ratio γ as design parameters, and the area-averaged adiabatic film cooling effectiveness η and the aerodynamic loss ξ as optimization objectives. The LHS method was used to generate 40 sample points in the design space, and numerical simulations were carried out to provide data for the training of the Kriging surrogate model. The maximum deviation between the area-averaged adiabatic film cooling effectiveness predicted by the Kriging surrogate model and the CFD simulation results was 2.35%, and the maximum deviation of the aerodynamic loss was 2.17%. Li et al. [123] used the radial basis function neural network (RBFNN) combined with the Non-dominated Sorting Genetic Algorithm II (NSGA-II) to perform multi-objective optimization on the LCS structure. Based on the numerical simulation results, the researchers explored the complex interaction between the film hole outflow gas and the mainstream. The Sobol method was used to analyze the influence of geometric parameters and external operating conditions on the double-wall cooling performance. The results showed that the optimized double-wall structure had a better film-coverage effect, and the comprehensive cooling performance was improved to a certain extent. Kim et al. [119] used the response surface method to conduct thermal analysis and optimization on the LCS structure. The surrogate model took the spacing between the impinging jet and the injection hole, the channel height from the impinging jet to the injection surface, the mass-flow ratio, and the mainstream temperature as design parameters, and the lowest thermal stress as the optimization objective. The results showed that the optimized design significantly reduced the thermal stress around the film cooling holes in the gas turbine components.

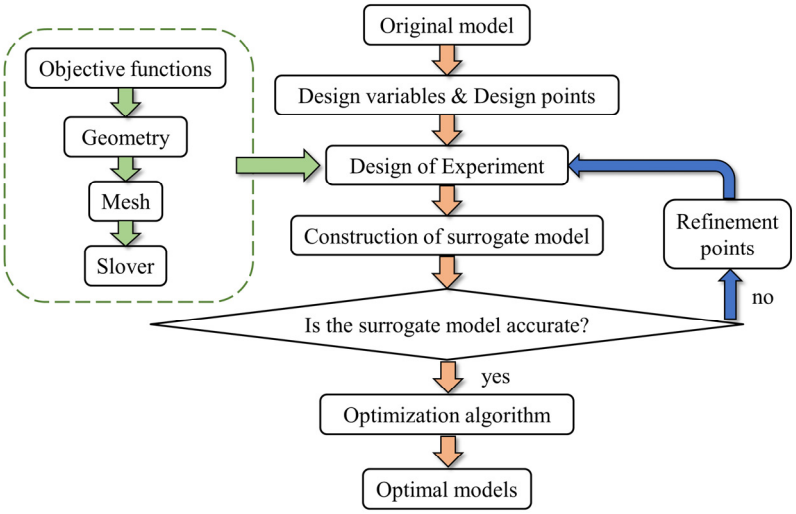

Figure 10. The optimization process using the surrogate model.

Deep learning (DL) emerged after 2012 and has made breakthrough progress in multiple fields. Specifically, it refers to machine learning (ML) based on deep neural network models and methods. It has developed on the basis of algorithmic models such as statistical machine learning and artificial neural networks (ANN), in combination with the development of contemporary big data and

high-computing power. Wang et al. [124] applied reinforcement learning to the intelligent optimization of the LCS. This method uses the Deep Q-Network (DQN) model for real-time optimization. The dataset consists of 246 groups of historical design data generated by CFD simulations and is extended by combining physical information. This intelligent model can achieve real-time optimization of the LCS in an average of 3 milliseconds, mainly due to the reward and punishment mechanisms set in reinforcement learning. The research results show that this intelligent optimization method can effectively reduce the thermal stress in turbine blades and improve cooling performance. Table 5 collates the optimization information for LCS optimization using the agent model.

Table 5. Optimization information for LCS optimization using surrogate models.

Ref.	Year	Optimization object	Surrogate model	Design parameter	Optimization target
Lv [87]	2022	A specific laminated cooling structure	Kriging	Hole diameter, Hole flow spacing, Hole spread spacing, and Porous plate thickness	η
Liu [122]	2025	A novel laminated cooling structure with pin-fins and slot hole	Kriging	Slot height s, Stream-wise inclination angle α, Diameter of the impingement hole, and Pin-fin filling ratio γ	η and Aerodynamic loss ξ
Li [123]	2023	Double-wall cooling structure	RBFNN	Impact hole diameter, Impact distance, Film hole diameter, Number of hole rows and columns	η and Pressure drop ΔP
Kim [119]	2014	Impingement/effusion cooling system	Response surface model	Ratio of hole spacing to hole diameter, Ratio of channel height to hole diameter, Mass flow rate ratio, and Mainstream temperature	Lowest thermal stress
Wang [124]	2024	Laminated cooling configurations	DQN	Diameter of the film and impact holes, Distance between the film holes, and Temperature of the main inlet	Coolant mass flow rate and Average temperature of the outer wall surface of the film plate

In addition, deep learning models represented by convolutional neural networks (CNN) show great advantages in the reconstruction of high-dimensional data information. Abundant two-dimensional/three-dimensional information can be directly used as the input or output of the model in the deep learning framework. This feature can help improve the fidelity of turbine cooling design and generate new research ideas for multiple local design problems. For example, Yang et al. [125] modeled the cooling efficiency distribution of transpiration cooling with arbitrary hole arrangements. Moreover,

in turbine cooling problems, flow and heat transfer problems with clear upstream-downstream relationships are often encountered. Recurrent neural networks (RNN) are a better means for such problems [126]. However, the application of current deep learning algorithms in the intelligent optimization design of the LCS is still in the development stage, and the construction of surrogate models mainly relies on common ML algorithms such as ANN.

4.2. Multi-objective optimization algorithms

Based on the trained surrogate model, a multi-objective optimization algorithm is used to find the optimum in the design space. Optimization of laminated cooling often requires design and decision-making problems with multiple design objectives that are often in opposition to each other, in which case a design solution that satisfies the multiple objectives needs to be found. Such optimization problems with more than one optimization objective that need to be handled simultaneously become multi-objective optimization problems (MOP). MOP belongs to the multi-criteria decision-making field [127], which means that when there are multiple objectives in a certain problem, due to the conflict between the objectives, the optimization of one objective may lead to the deterioration of the other objectives, so it is impossible to make multiple objectives reach the optimal value at the same time, and instead, coordination and compromise between the objectives are made to make the overall objective as optimal as possible. Unlike the unique solution of single-objective optimization, the MOP solution is usually a set of equilibrium solutions, a multitude of Pareto-optimal solutions. The solutions can be characterized, with the exception for the solutions on this set, no other solution can be found that is simultaneously better than all the objective functions sought. When there are multiple objectives, the solution that necessarily weakens at least one other objective function while improving any objective function is called a Pareto solution due to the phenomenon of conflicting and incomparable objectives [128]. In the absence of subjective preferences, all Pareto solutions are considered equally advantageous. Different solution ideas exist for solving multi-objective problems, such as finding only a set of Pareto optimal solutions that satisfy the requirements in a standard library function test, or quantitatively analyzing the level of importance between different objectives, or finding a solution that meets the subjective preferences of the decision maker as well as the experience of the decision maker in an engineering application [129].

Multi-objective optimization algorithms can be broadly classified into two categories: Direct search methods and stochastic search methods. Considering the complexity of the real-world problem, the stochastic search method is mainly applied in the laminated cooling optimization process. The common multi-objective stochastic algorithms are multi-objective genetic algorithm (MOGA) [130], second-generation non-dominated sequential genetic algorithm (NSGA-II) [131], and particle swarm optimization (PSO) [132].

Genetic algorithm (GA) is an optimization and search algorithm based on the principles of natural selection and genetics. The flowchart of the operations of the GA is given in Figure 11. MOGA is an extended GA-based algorithm that needs to take into account the multi-objective characteristics to ensure that the generated progeny performs well on multiple objectives, has global search capability, and can handle discrete variables [133]. Wang et al. [134] performed a multi-objective optimization of a specific LCS to improve its overall cooling effect and reduce the pressure drop under representative gas heat conditions in the combustion chamber. By using combined heat transfer CFD analysis and RBFNN model and GA, the optimal geometrical parameters were determined and two optimized

cooling structures for laminated cooling were proposed for maximizing the space-averaged overall cooling effect and minimizing the relative total pressure drop, respectively, in a given design space. In addition, the researchers explored the thermal stress distribution of the cooling structure and found a regular relationship between the thermal stresses and the overall cooling effect. Ismayilov et al. [135] performed a multi-objective optimization of the dimensions and the angle of attack of an airfoil shaped pin fins using MOGA, and the optimization resulted in the maximization of the cooling coefficient and the minimization of the pressure drop. The optimization results in bird-shaped pin fins with a novel cross-section, whose cooling coefficient is increased by 11.9% compared to the original wing-shaped pin fins, and the pressure drop is increased by only 7.3%.

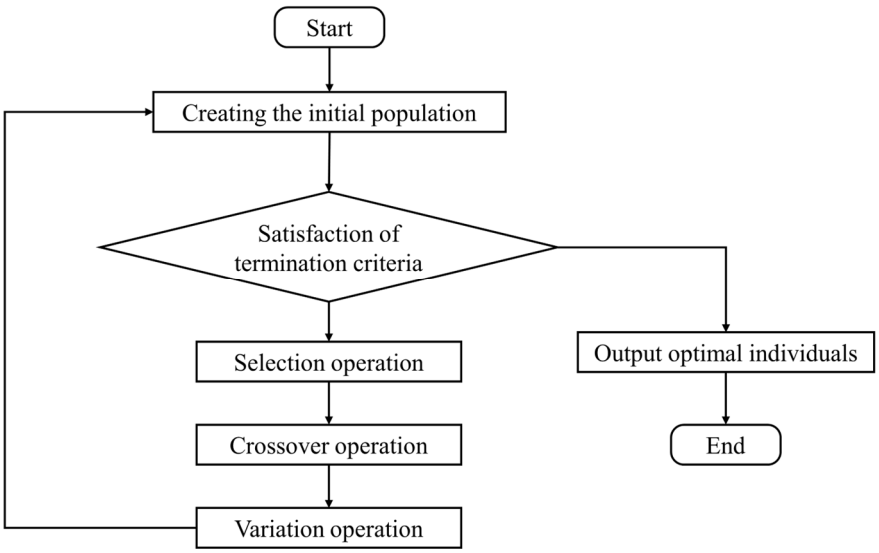

Figure 11. Flowchart of genetic algorithm.

NSGA-II is a genetic algorithm for solving MOPs, which is an improved version of NSGA that introduces the elite retention strategy, congestion comparison method, and optimal retention strategy. It largely improves the convergence speed of the iterations reduces the computational complexity [136]. Moon et al. [137] performed a multi-objective optimization of fan-shaped pin fins using the NSGA-II algorithm with the objective of maximizing heat transfer and minimizing friction losses. In the optimization process, LHS was used to generate 15 design points and the values of the objective function were evaluated at these points. The Pareto-optimal solution for the scalloped spoiler pin fins shows that the scalloped spoiler design improves in terms of heat transfer and pressure drop compared to the circular and reference pin fins. Figure 12 illustrates Moon's multi-objective optimization process. Li and Kim [138] conducted a multi-objective optimization of elliptical pin fins for a forked row using the NSGA-II algorithm. The geometric parameters of the pin fins are to be treated as design variables, the Nu and friction factor are used as optimization objectives. The results show that the average Nu obtained for the optimal shape is 87.8% and 12.8% larger than the reference shape and the circular shape, respectively.

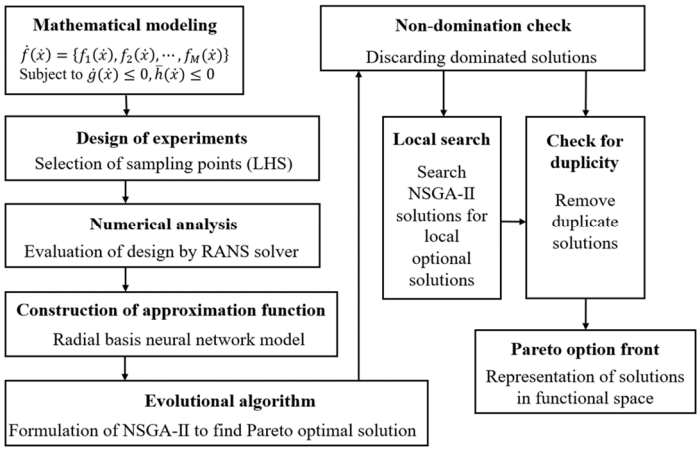

Figure 12. Multi-objective optimization process using LHS and NSGA-II.

To improve the accuracy in the process of spatial optimization, the representativeness and accuracy of the Pareto solution set can be effectively improved by combining the agent model with the multi-objective optimization algorithm. Nguyen et al. [139] optimized the shape of the pin fins in the cooling channel using GA and ML, an algorithm that can be used to automatically search for the shape of the pin fins. Through their optimization, they identified funnel-shaped pin fins, which increased the heat transfer coefficient by about 20% compared to standard circular pin fins without a significant increase in pressure drop losses. Jahromi et al. [140] conducted a comprehensive parametric study and multi-objective optimization of jet array impingement cooling with the aim of providing uniform cooling to the mid-chord section of gas turbine blades while reducing the consumption of air compression power. Three high-precision alternative models were developed through ANN to estimate key performance indicators, and Sobol global sensitivity analysis was applied to quantify the effects of design variables. Finally, the NSGA-II algorithm is used for optimization to obtain the optimal Pareto front under different desired Nusselt numbers, which provides an effective optimization scheme for the design of gas turbine blade cooling technology. Table 6 lists the details of the optimization cases mentioned in this section.

Table 6. Details of the optimization cases mentioned in this section.

Ref.	Year	Optimization object	Optimization method	Evaluation metric
Li [138]	2008	staggered elliptic-shaped short pin fin arrays	RANS + GRSM + EA	Nu and friction factor
Moon [137]	2014	a novel cross-sectional pin–fin shape	RANS + LES + MOEA + NSGA-II	Nu and friction factor
Wang [134]	2020	a specific laminated cooling structure	RANS + RBFNN + LHS + GA	spatially averaged η and C_p
Ismayilov [135]	2021	hydrofoil shaped pin fins	CFD + MOGA	HTC and C_p
Nguyen [139]	2023	pin fins array in a cooling channel	CFD + GA + ML	HTC and C_p
Jahromi [140]	2024	turbine blade array impingement structure	RANS + ANN + NSGA-II	compression power, $\overline{Nu}_s$, and uniformity index

By assisting the structural design of gas turbines through multi-objective optimization techniques, the advantages of more efficient heat transfer, more energy-efficient operation, lower cost, and better reliability can be achieved in many aspects. This can not only improve the overall performance of heat transfer systems and decrease energy consumption, but also promote the innovation and development of heat transfer. In the future, as the heat transfer field continues to deepen and expand, the application of optimization technology in the field of heat transfer will be more promising. By comprehensively considering a variety of different heat transfer objectives and constraints, researchers can utilize multi-objective techniques to discover more innovative and superior performance heat transfer solutions. Due to the many influencing factors of laminated cooling and the complexity of the optimization objectives, previous studies could not achieve a balanced approach and lacked a comprehensive assessment. The research on multi-objective optimization techniques in hot-end components of gas turbines is more in turbine blades, and almost no one has applied the optimization technique to LCS on the liner wall. However, its application in this field is very promising for subsequent development. Therefore, the multi-objective optimization technique in the optimization of combustion chamber liner structure is considered to be a hot spot of cutting-edge research and will receive more attention and exploration in the future.

4.3. Summarize the optimization process of LCS

We summarize the research methods and processes of LCS optimization through the literature research in the previous chapters as follows:

(1) The scope and objectives of the optimization problem are clarified by analyzing the deficiencies based on the structure. This usually includes improving the overall cooling efficiency, reducing the amount of cooling air used, reducing the pressure loss due to cooling airflow, and maintaining the uniformity of temperature distribution.

(2) Create a parametric geometric model of the LCS to facilitate the simulation of parameter variations. Select key geometric parameters that affect cooling performance, such as the aspect ratio of air film holes and impingement holes, the diameter and arrangement of the pin fins, or customized parameters that are added using shaped holes or shaped pin fins. Also define the range of design variables and engineering constraints such as minimum clearance, maximum thickness, etc.

(3) The collection of training data is used as input to the optimization algorithm. Due to the large amount of data, these data are often obtained through numerical simulations. For heat transfer studies, numerical simulations are performed using CFD software to measure the cooling performance under different geometric parameter configurations. Among other things, boundary and initial conditions for the CFD simulation need to be set up, including parameters for the prevailing velocity, temperature, pressure, and cooling air. Additional experiments are required to verify the validity of the numerical method.

(4) Adopt appropriate sampling strategies, such as LHS, to ensure uniform sampling of the design space. Train the model using training set data and improve the prediction accuracy of the model by adjusting the parameters to balance different optimization objectives. Analyze the degree of influence of different geometric parameters on the optimization objectives to identify key design variables.

(5) Appropriate surrogate models are used to train the prediction platform according to the specific requirements of the actual problem, such as the response surface model, Kriging model, neural network, to provide the basis for the subsequent multi-objective spatial optimization.

(6) Select algorithms suitable for multi-objective optimization, such as MOGA, NSGA-II and PSO, and incorporate advanced intelligence techniques, such as AI and ML, which are used to find the optimal Pareto solution set in the multi-dimensional parameter space.

(7) Verify the accuracy of the optimization model through experimental data or numerical simulations with higher fidelity, assess the trade-offs and feasibility of various optimization schemes under different conditions, propose further improvements and research directions, and conduct multiple design iterations based on the results. Based on the optimization results and actual engineering requirements, the final LCS design is selected.

5. Conclusions and outlook

We provide a comprehensive review of the optimization efforts related to laminated cooling structure (LCS) for gas turbines, including experimental and numerical simulation studies, analysis of the influencing factors and optimization objectives, advantages, and process of multi-objective optimization techniques. The principal conclusions are as follows:

(1) The experiments and simulations of LCS mainly reveal the effects of changes in geometrical structure parameters on its flow loss and wall heat transfer law and cooling effect. Test methods commonly used in experiments include infrared thermal imaging and transient liquid crystal measurement techniques. Numerical simulation is commonly used in the RANS method, considering the fluid-structure interaction effect. The SST $k-\omega$ model is deemed most effective for simulating LCS with complex channel structure.

(2) When optimizing the structure of the film holes, the optimum structural parameters are influenced by the blowing ratio. The film cooling efficiency increases and then decreases with the increase of blowing ratio. Smaller *L/D* of film holes in LCS leads to lower adiabatic film cooling efficiency as well as higher near-wall heat transfer coefficient. Non-uniform pore size shows advantage in cooling uniformity.

(3) Internal cooling contributes significantly to the cooling performance and heat transfer capabilities. Pin fins arranged in a staggered and non-uniform pattern demonstrate excellent performance. Profiled pin fins improve heat transfer capabilities while reducing flow resistance, but they also increase the complexity of optimization and manufacturing.

(4) The selection of materials for LCS is also an aspect of optimization, and it is necessary to conduct research on composite material laminated cooling. The integration of LCS and TBC technology has the potential to significantly enhance the thermal protection of wall surfaces.

(5) Intelligent optimization algorithms facilitate the optimization of LCS. The primary multi-objective optimization methods are MOGA, NSGA-II, and PSO. Each of these methods has its own characteristics, and the most appropriate method needs to be determined in conjunction with the actual situation. The incorporation of advanced techniques, such as AM, TO, AI, and ML, can improve the efficiency and accuracy of optimization.

Based on the previous discussion and after summarizing the shortcomings of the existing studies, the authors believe that future work can be carried out in the following areas:

(1) It is necessary to construct a high-precision coupled fluid-heat calculation method for gas turbines in service environments based on existing experimental data. Although there is a mature research foundation, a more advanced and accurate comprehensive analysis is still worth studying.

In terms of the complementary relationship between numerical and experimental work: Experimentally, we can obtain real-world data on the flow and heat transfer characteristics of gas turbines under different operating conditions. These data can be used to validate and calibrate numerical models. For example, by measuring the temperature and pressure distributions on the surface of the gas turbine components through experimental setups, we can check if the numerical simulation results match the actual situation. Numerically, we can conduct parametric studies more conveniently. We can change the film hole parameters, pin fin parameters, spatial arrangement parameters, and flow parameters in the numerical model to predict their effects on the flow and heat transfer characteristics. Then, we can design more targeted experiments based on the numerical prediction results.

Researchers should focus on the comprehensive analysis based on experimental results and numerical calculations to reveal the correlation mechanism and quantitative correlation formula between the film holes parameters, pin fins parameters, spatial arrangement parameters, and flow parameters on the flow and heat transfer characteristics, and to deeply investigate the flow, and heat transfer influence law of laminated cooling.

(2) Existing research entails only the base form of a single cooled structure to optimize the size of regular shapes, of which there is little research on shaped structures. The development of additive manufacturing technology breaks through the limitations on the fabrication of complex shaped structures and provides support for topologically optimized structures.

Shaped holes such as cat's ear holes [141] and double-jet holes [142], and shaped pin fins such as annular pin fins [111] and Kagome trusses [112] possess excellent performance and can be applied to LCS. Cat's ear holes, for example, have a unique shape that can enhance the lateral spreading of the cooling air, improving the cooling effectiveness over a larger area. Double-jet holes can create a more complex flow pattern, which may lead to better mixing of the cooling air with the hot mainstream, thus enhancing heat transfer.

Annular pin fins can increase the surface area for heat transfer and also have a more uniform flow distribution around them compared to traditional pin fins. Kagome trusses, with their unique topological structure, can provide both good mechanical support and enhanced heat transfer performance. The application of these shaped structures in LCS requires further research on their manufacturing processes, flow and heat transfer characteristics, and optimization of their geometric parameters.

(3) Complex structures may improve cooling, but other effects may be overlooked. For example, the addition of new structures can lead to uneven cooling and may also weaken the structure. Studies have a single evaluation model, which may be one-sided for a holistic view of the overall performance of different laminate structures.

There is a need to introduce multiple evaluation indexes and utilize the cooling efficiency, temperature uniformity, pressure loss coefficient, and comprehensive impact factor for comprehensive research. Cooling efficiency is a direct indicator of how well the cooling structure can reduce the temperature of the hot components. Temperature uniformity reflects the evenness of the temperature distribution on the surface of the component, which is crucial for preventing thermal stress concentration. Pressure loss coefficient measures the energy loss caused by the cooling structure in the flow path.

Structural mechanical properties and manufacturing costs should also be considered. For example, when designing a new laminated cooling structure, we need to ensure that it can withstand the

mechanical loads during the operation of the gas turbine. Furthermore, the manufacturing cost should be kept within an acceptable range. By considering these factors, we can design more reasonable and practical laminated cooling structures.

(4) The application of multi-objective optimization technology in the structural design of gas turbines is promising. At present, the multi-objective optimization of LCS is in its infancy, and most are optimized on the turbine blades; thus, researchers can conduct targeted multi-objective optimization research on the liner LCS under combustion chamber conditions.

To establish a systematic optimization framework for future LCS research, we need to define a comprehensive objective function that includes multiple performance indexes such as cooling efficiency, temperature uniformity, pressure loss coefficient, structural mechanical properties, and manufacturing costs. This objective function will serve as the basis for optimization. Second, we should integrate different types of data sources, including experimental data, numerical simulation data and historical design data. These data can be used to train machine learning models and improve the accuracy of optimization algorithms. Third, we need to develop an iterative optimization process. In each iteration, the optimization algorithm adjusts the design parameters of the LCS based on the objective function and the data, and then evaluates the performance of the new design through numerical simulation or experiments.

It is also necessary to improve the efficiency and accuracy of multi-objective optimization algorithms, explore the application of machine learning and artificial intelligence in LCS optimization, and promote the intelligence and automation of design optimization. More than that, by combining data, algorithms, and hardware, mining the optimal structural design principles under the response of each performance index, and strengthening the overall design and integration research of the laminated cooling system, a structural design platform based on optimization algorithms can be developed, and LCS design and analysis software for performance prediction can be developed.

Use of AI tools declaration

The authors declare they have not used Artificial Intelligence (AI) tools in the creation of this article.

Acknowledgments

This work was supported by the State Key Laboratory of Clean and Efficient Turbomachinery Power Equipment Open Topic Grant (DEC8300CG202417650A1228128).

Conflict of interest

The authors declare no conflicts of interest.

Author contributions

Conceptualization, X.T. (Xiaojing Tian) and W.Y. (Weiqi Ye); methodology, W.Y.; validation, L.H. (Langming Huang) and S.J. (Shenglong Jin); formal analysis, L.X. (Liang Xu); investigation, W.Y.; resources, X.T. and A.Y. (Anjian Yang); data curation, W.Y.; writing—original draft preparation, W.Y; writing—review and editing, L.X. and S.J.; visualization, W.Y; supervision, X.T. and L.X; project

administration, A.Y. and L.H.; funding acquisition, L.X.. All authors have read and agreed to the published version of the manuscript.

References

1. Han JC, Dutta S, Ekkad S (2013) Gas turbine heat transfer and cooling technology. 2nd Edition, CRC press, 887. https://doi.org/10.1201/b13616
2. Xu L, Sun Z, Ruan Q, et al. (2023) Development trend of cooling technology for turbine blades at super-high temperature of above 2000 K. *Energies* 16: 668. https://doi.org/10.3390/en16020668
3. Fujita D, Miyazaki T (2024) Techno-economic analysis on the balance of plant (BOP) equipment due to switching fuel from natural gas to hydrogen in gas turbine power plants. *AIMS Energy* 12: 464–480. https://doi.org/10.3934/energy.2024021
4. Han JC (2018) Advanced cooling in gas turbines 2016 Max jakob memorial award paper. *J Heat Transfer,* 140. https://doi.org/10.1115/1.4039644
5. Zhang T, Zhang Y, Katterbauer K, et al. (2024) Deep learning-assisted phase equilibrium analysis for producing natural hydrogen. *Int J Hydrogen Energy* 50: 473–486. https://doi.org/10.1016/j.ijhydene.2023.09.097
6. Qian X, Yan P, Wang X, et al. (2023) Effect of thermal barrier coatings and integrated cooling on the conjugate heat transfer and thermal stress distribution of nickel-based superalloy turbine vanes. *Energy* 277: 127774. https://doi.org/10.1016/j.energy.2023.127774
7. Niu JJ, Liu CL, Fu S, et al. (2022) Experiment investigation of impingement/effusion cooling on overall cooling effectiveness and temperature gradients of afterburner heat shields in a high-performance aircraft engine. *Exp Therm Fluid Sci* 139: 110698. https://doi.org/10.1016/j.expthermflusci.2022.110698
8. Denton JD (1993) The 1993 IGTI scholar lecture: Loss mechanisms in turbomachines. *J Turbomach* 115: 621–656. https://doi.org/10.1115/1.2929299
9. Wassell AB, Bhangu JK (2015) The development and application of improved combustor wall cooling techniques. *Proceedings of the ASME 1980 International Gas Turbine Conference and Products Show, 1A: General*. New Orleans, Louisiana, USA. March 10–13, 1980. https://doi.org/10.1115/80-GT-66
10. Liu Y, Sun X, Sethi V, et al. (2017) Review of modern low emissions combustion technologies for aero gas turbine engines. *Progress Aerospace Sci* 94: 12–45. https://doi.org/10.1016/j.paerosci.2017.08.001
11. Azad GS, Huang Y, Han JC (2000) Impingement heat transfer on dimpled surfaces using a transient liquid crystal technique. *J Therm Heat Transfer* 14: 186–193. https://doi.org/10.2514/2.6530
12. Chyu MK, Siw SC (2013) Recent Advances of internal cooling techniques for gas turbine airfoils. *J Therm Sci Eng Appl* 5: 021008. https://doi.org/10.1115/1.4023829
13. Wei C, Vasquez Diaz GA, Wang K, et al. (2020) 3D-printed tubes with complex internal fins for heat transfer enhancement—CFD analysis and performance evaluation. *AIMS Energy* 8: 27–47. https://doi.org/10.3934/energy.2020.1.27
14. Yeranee K, Rao Y (2021) A review of recent studies on rotating internal cooling for gas turbine blades. *Chinese J Aeronaut* 34: 85–113. https://doi.org/10.1016/j.cja.2020.12.035

15. Bunker RS (2010) Film cooling: Breaking the limits of diffusion shaped holes. *Heat Transfer Res* 41: 627–650. http://dx.doi.org/10.1615/HeatTransRes.v41.i6.40
16. Zhang J, Zhang S, Wang C, et al. (2020) Recent advances in film cooling enhancement: A review. *Chinese J Aeronaut* 33: 1119–1136. https://doi.org/10.1016/j.cja.2019.12.023
17. He Z, Huang T, Bao Z, et al. (2024) Research on optimization of combustor liner structure based on arc-shaped slot hole. *Open Physic* 22: 20240072. https://doi.org/10.1515/phys-2024-0072
18. Dutta S, Kaur I, Singh P (2022) Review of film cooling in gas turbines with an emphasis on additive manufacturing-based design evolutions. *Energies* 15: 6968. https://doi.org/10.3390/en15196968
19. Panda RK, Pujari AK, Gudla B (2024) Flow structure comparison of film cooling versus hybrid cooling: A CFD study. *Int J Turbo Jet-Engines* 41: 227–240. https://doi.org/10.1515/tjj-2022-0058
20. Wang L, Lv C, Mao J, et al. (2024) Influence mechanism of impingement and film on the flow and heat transfer of turbine outer ring with composite cooling structure under different operating parameters. *Appl Therm Eng* 246: 122883. https://doi.org/10.1016/j.applthermaleng.2024.122883
21. Li W, Lu X, Li X, et al. (2019) On improving full-coverage effusion cooling efficiency by varying cooling arrangements and wall thickness in double wall cooling application. *J Heat Transfer* 141: 042201. https://doi.org/10.1115/1.4042772
22. Colladay RS (1972) Analysis and comparison of wall cooling schemes for advanced gas turbine applications. Washington, D.C., National Aeronautics and Space Administration. http://catalog.hathitrust.org/Record/011445003
23. Nealy DA, Reider SB (1980) Evaluation of laminated porous wall materials for combustor liner cooling. *J Eng Power* 102: 268–276. https://doi.org/10.1115/1.3230247
24. Hess WG (1979) Laminated turbine vane design and fabrication. No. FR-11662. Available from: https://ntrs.nasa.gov/citations/19790025033.
25. Ashmole P (1983) Introducing the Rolls-Royce tay. *19th Joint Propulsion Conference*, 1377. https://doi.org/10.2514/6.1983-1377
26. Mongia H, Reider S (1985) Allison combustion research and development activities. *AIAA/SAE/ASME/ASEE 21st Joint Propulsion Conference.* Available from: https://jglobal.jst.go.jp/en/detail?JGLOBAL_ID=200902092009449055.
27. Bunker RS (2013) Gas turbine cooling: Moving from macro to micro cooling. *ASME Turbo Expo 2013: Turbine Technical Conference and Exposition*: V03CT14A002. https://doi.org/10.1115/GT2013-94277
28. Bunker RS (2017) Evolution of turbine cooling. *ASME Turbo Expo 2017: Turbomachinery Technical Conference and Exposition*: V001T51A001. https://doi.org/10.1115/GT2017-63205
29. Kim I, Jin H, Ri K, et al. (2024) Design methodology for combustor in advanced gas turbine engines: A review. *Aircr Eng Aerosp Technol* 96: 285–296. https://doi.org/10.1108/aeat-12-2022-0351
30. Zhang G, Zhu R, Xie G, et al. (2022) Optimization of cooling structures in gas turbines: A review. *Chinese J Aeronaut* 35: 18–46. https://doi.org/10.1016/j.cja.2021.08.029
31. Xu L, Jin S, Ye W, et al. (2024) A review of machine learning methods in turbine cooling optimization. *Energies* 17: 3177. https://doi.org/10.3390/en17133177
32. Zhu XD, Zhang JZ, Tan XM (2019) Numerical assessment of round-to-slot film cooling performances on a turbine blade under engine representative conditions. *Int Commun Heat Mass Transfer* 100: 98–110. https://doi.org/10.1016/j.icheatmasstransfer.2018.12.008

33. Wang J, Lv X, Liu Q, et al. (2009) An experimental investigation on cooling performance of a laminated configuration using infrared thermal image technique. *ASME Turbo Expo 2009: Power Land Sea Air*, 765–771. https://doi.org/10.1115/GT2009-59838
34. Wang W, Pu J, Wang JH, et al. (2019) An experimental investigation on cooling characteristics of a vane laminated end-wall with axial-row layout of film-holes. *Appl Therm Eng* 148: 953–962. https://doi.org/10.1016/j.applthermaleng.2018.11.104
35. Aga V, Mansour M, Abhari RS (2009) Aerothermal performance of streamwise and compound angled pulsating film cooling jets. *J Turbomach* 131: 041015. https://doi.org/10.1115/1.3072489
36. Zhang R, Luo C, Zhou L, et al. (2022) Impingement/film cooling of C3X vane with double-wall cooling structure using air/mist mixture. *Int J Heat Mass Transfer* 188: 122594. https://doi.org/10.1016/j.ijheatmasstransfer.2022.122594
37. Bunker RS, Bailey JC (2001) Film cooling discharge coefficient measurements in a turbulated passage with internal crossflow. *J Turbomach* 123: 774–780. https://doi.org/10.1115/1.1397307
38. Ji Y, Singh P, Ekkad SV, et al. (2017) Effect of crossflow regulation by varying jet diameters in streamwise direction on jet impingement heat transfer under maximum crossflow condition. *Numer Heat Transfer Part A* 72: 579–599. https://doi.org/10.1080/10407782.2017.1394136
39. Zhou J, Tian J, Lv H, et al. (2022) Numerical investigation on flow and heat transfer characteristics of single row jet impingement cooling with varying jet diameter. *Int J Therm Sci* 179: 107710. https://doi.org/10.1016/j.ijthermalsci.2022.107710
40. Yao R, Liu T, Huang X, et al. (2023) Multi-objective design of laminated cooling configuration applied in gas turbine based on fuzzy grey relational analysis. *Int J Heat Mass Transfer* 207: 124035. https://doi.org/10.1016/j.ijheatmasstransfer.2023.124035
41. Sweeney PC, Rhodes JF (1999) An infrared technique for evaluating turbine airfoil cooling designs. *J Turbomach* 122: 170–177. https://doi.org/10.1115/1.555438
42. Nakamata C, Mimura F, Matsushita M, et al. (2007) Local cooling effectiveness distribution of an integrated impingement and pin fin cooling configuration. *Proc ASME Turbo Expo 2007: Power Land Sea Air* 4: 23–34. https://doi.org/10.1115/GT2007-27020
43. Wang JH, Xu HZ, Liu YL, et al. (2008) Experimental and numerical investigations on turbine airfoil cooling designs: Part I—An investigation on flow features by particle image velocimetry. *ASME Turbo Expo 2008: Power Land Sea Air* 4: 635–641. https://doi.org/10.1115/GT2008-50673
44. Kim SH, Ahn KH, Jung EY, et al. (2014) Total cooling effectiveness on laminated multilayer for impingement/effusion cooling system. *ASME Turbo Expo 2014: Turbine Tech Conf Exposition* 5B: V05BT13A050. https://doi.org/10.1115/GT2014-26692
45. Wang W, Pu J, Yuan RM, et al. (2017) An experimental investigation on the overall cooling performances of two turbine end-wall structures. *Proc ASME Turbo Expo 2017: Turbomachinery Tech Conf Exposition* 5C: V05CT19A005. https://doi.org/10.1115/GT2017-63226
46. Pu J, Wang W, Wang JH, et al. (2020) Experimental study of free-stream turbulence intensity effect on overall cooling performances and solid thermal deformations of vane laminated end-walls with various internal pin–fin configurations. *Appl Therm Eng* 173: 115232. https://doi.org/10.1016/j.applthermaleng.2020.115232
47. Pu J, Zhang T, Wang JH (2022) Experimental study of cooling air effect on overall cooling of laminated configuration at a turbine vane end-wall. *Case Studies Therm Eng* 32: 101890. https://doi.org/10.1016/j.csite.2022.101890

48. Bai N, Fan W, Zhu J, et al. (2023) Experimental investigations into the effusion plate wall temperature of impingement/effusion cooling systems for gas turbine combustors. *Aerosp Sci Technol* 132: 108052. https://doi.org/10.1016/j.ast.2022.108052
49. Funazaki K, Tarukawa Y, Kudo T, et al. (2001) Heat transfer characteristics of an integrated cooling configuration for ultra-high temperature turbine blades: Experimental and numerical investigations. *Proc ASME Turbo Expo 2001: Power Land Sea Air* 3: V003T01A031. https://doi.org/10.1115/2001-GT-0148
50. Manzhao K, Huiren Z, Songling L, et al. (2008) Internal heat transfer characteristics of lamilloy configurations. *Chinese J Aeronaut* 21: 28–34. https://doi.org/10.1016/S1000-9361(08)60004-7
51. Terzis A, Ott P, Cochet M, et al. (2014) Effect of varying jet diameter on the heat transfer distributions of narrow impingement channels. *J Turbomach* 137: 021004. https://doi.org/10.1115/1.4028294
52. Zhang W, Zhu H, Li G, et al. (2016) Experimental investigation on flow resistance and heat transfer coefficient of internal lamilloy. *ASME Turbo Expo 2016: Turbomachinery Technical Conference and Exposition* V05BT16A001. https://doi.org/10.1115/GT2016-56105
53. Batchelor GK (2000) An introduction to fluid dynamics. Cambridge University Press, 131–173. https://doi.org/10.1017/CBO9780511800955
54. Moin P, Mahesh K (1998) Direct numerical simulation: a tool in turbulence research. *Annu Rev Fluid Mech* 30: 539–578. https://doi.org/10.1146/annurev.fluid.30.1.539
55. Wilcox DC (2006) Turbulence modeling for CFD. La Canada, CA: DCW industries, (third edition), 73–135. Avaiable from: https://www.amazon.com/Turbulence-Modeling-CFD-Third Edition/dp/1928729088.
56. Fureby C, Grinstein FF (2002) Large eddy simulation of high-reynolds-number free and wall-bounded flows. *J Comput Phys* 181: 68–97. https://doi.org/10.1006/jcph.2002.7119
57. Chaouat B (2017) The state of the art of hybrid rans/les modeling for the simulation of turbulent flows. *Flow Turbul Combust* 99: 279–327. https://doi.org/10.1007/s10494-017-9828-8
58. Gong C, Zhao S, Chen W, et al. (2023) Numerical study on the combustion process in a gas turbine combustor with different reference velocities. *Adv Aerodyn* 5: 24. https://doi.org/10.1186/s42774-023-00154-0
59. Funazaki K, Hachiya K (2003) Systematic numerical studies on heat transfer and aerodynamic characteristics of impingement cooling devices combined with pins. *ASME Turbo Expo 2003, collocated with the 2003 International Joint Power Generation Conference* 5: 185–192. https://doi.org/10.1115/GT2003-38256
60. Funazaki KI, Bin Salleh H (2008) Extensive studies on internal and external heat transfer characteristics of integrated impingement cooling structures for hp turbines. *ASME Turbo Expo 2008: Power Land Sea Air* 4: 167–176. https://doi.org/10.1115/GT2008-50202
61. Panda RK, Prasad BVSSS (2012) Conjugate heat transfer from a flat plate with combined impingement and film cooling. *ASME Turbo Expo 2012: Turbine Technical Conference and Exposition.* 4: 347–356. https://doi.org/10.1115/GT2012-68830
62. Gao W, Li H, Li L, et al. (2021) Numerical simulation of broken pin effects on the flow field and cooling performance of a double-wall cooling configuration. *Chinese J Aeronaut* 34: 358–375. https://doi.org/10.1016/j.cja.2020.09.014

63. Nakamata C, Okita Y, Matsuno S, et al. (2005) Spatial arrangement dependance of cooling performance of an integrated impingement and pin fin cooling configuration. *ASME Turbo Expo 2005: Power Land Sea Air* 3: 385–395. https://doi.org/10.1115/GT2005-68348
64. Rao Y, Liu Y, Wan C (2018) Multiple-jet impingement heat transfer in double-wall cooling structures with pin fins and effusion holes. *Int J Therm Sci* 133: 106–119. https://doi.org/10.1016/j.ijthermalsci.2018.07.021
65. Bohn DE, Tu¨mmers C (2003) Numerical 3-D conjugate flow and heat transfer investigation of a transonic convection-cooled thermal barrier coated turbine guide vane with reduced cooling fluid mass flow. *Proc ASME Turbo Expo 2003, Collocated 2003 Int Joint Power Gener Conf* 5: 279–286. https://doi.org/10.1115/GT2003-38431
66. Zhou W, Deng Q, Feng Z (2016) Conjugate heat transfer analysis for laminated cooling effectiveness: Part A—Effects of surface curvature. *ASME Turbo Expo 2016: Turbomachinery Technical Conference and Exposition* 5A: V05AT10A008. https://doi.org/10.1115/GT2016-57243
67. Deng Q, Zhou W, Feng Z (2016) Conjugate heat transfer analysis for laminated cooling effectiveness: Part B—Effects of film hole incline angle. *ASME Turbo Expo 2016: Turbomachinery Technical Conference and Exposition* 5A: V05AT10A009. https://doi.org/10.1115/GT2016-57256
68. Yang X, Liu Z, Zhao Q, et al. (2019) Conjugate heat transfer measurements and predictions for the vane endwall of a high-pressure turbine with upstream purge flow. *Int J Heat Mass Transfer* 140: 634–647. https://doi.org/10.1016/j.ijheatmasstransfer.2019.06.030
69. He J, Deng Q, Feng Z (2021) Conjugate heat transfer characteristics of double wall cooling with gradient diameter of film and impingement holes. *Proceedings of the ASME Turbo Expo 2021: Turbomachinery Technical Conference and Exposition* 5A: V05AT12A017. https://doi.org/10.1115/GT2021-59423
70. Skamniotis C, Courtis M, Cocks ACF (2021) Multiscale analysis of thermomechanical stresses in double wall transpiration cooling systems for gas turbine blades. *Int J Mech Sci* 207: 106657. https://doi.org/10.1016/j.ijmecsci.2021.106657
71. Zhang D, Liu H, Chen P, et al. (2024) Numerical analysis on multiple parameters for overall cooling effectiveness of impingement effusion cooling with low Reynolds number. *Int Commun Heat Mass Transfer* 153: 107366. https://doi.org/10.1016/j.icheatmasstransfer.2024.107366
72. Yeranee K, Rao Y, Xu C, et al. (2024) Conjugate heat transfer and fluid flow analysis on printable double-wall effusion cooling with internal topology-optimized TPMS structures. *Therm Sci Eng Progress* 55: 102939. https://doi.org/10.1016/j.tsep.2024.102939
73. Yeranee K, Rao Y, Zuo Q, et al. (2024) Thermal performance enhancement for gas turbine blade trailing edge cooling with topology-optimized printable diamond TPMS lattice. *Int J Heat Fluid Flow* 110: 109649. https://doi.org/10.1016/j.ijheatfluidflow.2024.109649
74. Zhang XD, Liu JJ, An BT (2016) The influences of element layout and coolant ejection angle on overall cooling effectiveness of laminated cooling configuration. *Int J Heat Mass Transfer* 101: 988–991. https://doi.org/10.1016/j.ijheatmasstransfer.2016.04.104
75. Song W, Xu H, Cheng X, et al. (2019) Numerical investigation on cooling air flow and resistance characteristics inner laminated cooling structures. *Proceedings of the ASME Turbo Expo 2019: Turbomachinery Technical Conference and Exposition* 5A: V05AT10A012. https://doi.org/10.1115/GT2019-92025

76. Liu R, Li H, You R, et al. (2022) Multi-parameters sensitivity analysis of overall cooling effectiveness on turbine blade and numerical investigation of internal cooling structures on heat transfer. *Proc ASME Turbo Expo 2022: Turbomachinery Tech Conf Exposition* 6A: V06AT12A026. https://doi.org/10.1115/GT2022-82372
77. Song W, Yao R, Wang J, et al. (2023) Transient film outflow performances of laminated cooling configurations in leading edges of turbine vane. *Appl Therm Eng* 233: 121209. https://doi.org/10.1016/j.applthermaleng.2023.121209
78. Tagawa GBS, Morency F, Beaugendre H (2021) CFD investigation on the maximum lift coefficient degradation of rough airfoils. *AIMS Energy* 9: 305–325. https://doi.org/10.3934/energy.2021016
79. Lei L, Wang C, Wang L, et al. (2015) Computational investigation of dimple effects on heat transfer and friction factor in a Lamilloy cooling structure. *J Enhanced Heat Transfer* 22: 147–175. https://doi.org/10.1615/JENHHEATTRANSF.2015013956
80. Luo L, Wang C, Wang L, et al. (2016) A numerical investigation of dimple effects on internal heat transfer enhancement of a double wall cooling structure with jet impingement. *Int J Numer Methods Heat Fluid Flow* 26: 2175–2197. https://doi.org/10.1108/HFF-02-2015-0081
81. Wang XY, Liu CL, Zhu HR, et al. (2024) Investigation on cooling characteristic of the novel double-wall with the hollow pin fin. *Int J Therm Sci* 195: 108647. https://doi.org/10.1016/j.ijthermalsci.2023.108647
82. Li H, Xie F, Wang Y, et al. (2022) Numerical investigation on the cooling effectiveness and pressure loss of a novel laminated cooling configuration with cellular partition. *J Therm Sci Eng Appl* 15: 011015. https://doi.org/10.1115/1.4055744
83. Chen Z, Chen X, Yang X, et al. (2024) Numerical study on cooling characteristics of turbine blade based on laminated cooling configuration with clapboards. *Energy* 299: 131372. https://doi.org/10.1016/j.energy.2024.131372
84. Gu H, Liang D, Duan P, et al. (2023) Aerothermal characteristics of thin double-wall effusion cooling systems with novel slot holes and cellular architectures for gas turbines. *Aerospace Sci Technol* 140: 108441. https://doi.org/10.1016/j.ast.2023.108441
85. Bang M, Kim S, Park HS, et al. (2021) Impingement/effusion cooling with a hollow cylinder structure for additive manufacturing: Effect of channel gap height. *Int J Heat Mass Transfer* 175: 121420. https://doi.org/10.1016/j.ijheatmasstransfer.2021.121420
86. Skamniotis C, Cocks ACF (2021) 2D and 3D thermoelastic phenomena in double wall transpiration cooling systems for gas turbine blades and hypersonic flight. *Aerospace Sci Technol* 113: 106610. https://doi.org/10.1016/j.ast.2021.106610
87. Lv Y, Liu T, Huang X, et al. (2022) Numerical investigation and optimization of flat plate transpiration-film combined cooling structure. *Int J Therm Sci* 179: 107673. https://doi.org/10.1016/j.ijthermalsci.2022.107673
88. Haven BA, Kurosaka M (1997) Kidney and anti-kidney vortices in crossflow jets. *J Fluid Mechanics* 352: 27–64. https://doi.org/10.1017/S0022112097007271
89. Baldauf S, Scheurlen M, Schulz A, et al. (2002) Correlation of film-cooling effectiveness from thermographic measurements at enginelike conditions. *J Turbomach* 124: 686–698. https://doi.org/10.1115/1.1504443

90. Li W, Li X, Ren J, et al. (2018) Length to diameter ratio effect on heat transfer performance of simple and compound angle holes in thin-wall airfoil cooling. *Int J Heat Mass Transfer* 127: 867–879. https://doi.org/10.1016/j.ijheatmasstransfer.2018.08.086
91. Li W, Lu X, Li X, et al. (2018) High resolution measurements of film cooling performance of simple and compound angle cylindrical holes with varying hole length-to-diameter ratio—Part I: Adiabatic film effectiveness. *Int J Therm Sci* 124: 146–161. https://doi.org/10.1016/j.ijthermalsci.2017.10.013
92. Ignatious I, Janardanan Sarasamma J (2015) Numerical analysis of impingement/effusion cooling effectiveness on flat plates. *Proceedings of the ASME 2015 Gas Turbine India Conference. ASME 2015 Gas Turbine India Conference*: V001T04A004. https://doi.org/10.1115/GTINDIA2015-1319
93. Burd SW, Kaszeta RW, Simon TW (1998) Measurements in film cooling flows: Hole L/D and turbulence intensity effects. *J Turbomach* 120: 791–798. https://doi.org/10.1115/1.2841791
94. Lutum E, Johnson BV (1999) Influence of the hole length-to-diameter ratio on film cooling with cylindrical holes. *J Turbomach* 121: 209–216. https://doi.org/10.1115/1.2841303
95. Li X, He Y, Mao R, et al. (2014) Experimental investigations on cooling hole diameters of an impingement-effusion cooling system. *Proceedings of the ASME Turbo Expo 2014: Turbine Technical Conference and Exposition* 5B: V05BT14A016. https://doi.org/10.1115/GT2014-26521
96. Zhou W, Deng Q, He W, et al. (2017) Effects of hole pitch to diameter ratio P/D of impingement and film hole on laminated cooling effectiveness. *Proceedings of the ASME Turbo Expo 2017: Turbomachinery Technical Conference and Exposition.* 5A: V05AT10A005. https://doi.org/10.1115/GT2017-64566
97. Liu Y, Rao Y, Yang L (2020) Numerical simulations of a double-wall cooling with internal jet impingement and external hexagonal arrangement of film cooling holes. *Int J Therm Sci* 153: 106337. https://doi.org/10.1016/j.ijthermalsci.2020.106337
98. Li H, Li L, Li Q, et al. (2023) Coupling characteristics and simplification analysis method of laminated cooling configuration between external and internal cooling. *Int J Therm Sci* 187: 108159. https://doi.org/10.1016/j.ijthermalsci.2023.108159
99. Viskanta R (1993) Heat transfer to impinging isothermal gas and flame jets. *Exp Therm Fluid Sci* 6: 111–134. https://doi.org/10.1016/0894-1777(93)90022-B
100. Wang C, Wang C, Zhang J (2021) Parametric studies of laminated cooling configurations: Overall cooling effectiveness. *Int J Aerosp Eng* 2021: 6656804. https://doi.org/10.1155/2021/6656804
101. Wang C, Zhang X, Hu K, et al. (2023) Geometric-parameter influence and orthogonal evaluation on the thermal environment for an impinging jet ventilation system inlet. *Case Stud Therm Eng* 51: 103573. https://doi.org/10.1016/j.csite.2023.103573
102. Xu F, Pan Z, Wu H (2017) Experimental investigation on the flow transition in different pin-fin arranged microchannels. *Microfluid Nanofluid* 22: 11. https://doi.org/10.1007/s10404-017-2030-4
103. Bianchini C, Facchini B, Simonetti F, et al. (2010) Numerical and experimental investigation of turning flow effects on innovative pin fin arrangements for trailing edge cooling configurations. *Proc ASME Turbo Expo 2010: Power Land Sea Air* 4: 593–604. https://doi.org/10.1115/GT2010-23536
104. Abuşka M, Çorumlu V (2023) A comparative experimental thermal performance analysis of conical pin fin heat sink with staggered and modified staggered layout under forced convection. *Therm Sci Eng Prog* 37: 101560. https://doi.org/10.1016/j.tsep.2022.101560

105. Bahiraei M, Mazaheri N, Daneshyar MR (2021) Employing elliptical pin-fins and nanofluid within a heat sink for cooling of electronic chips regarding energy efficiency perspective. *Appl Therm Eng* 183: 116159. https://doi.org/10.1016/j.applthermaleng.2020.116159
106. Ostanek JK, Thole KA (2013) Effects of non-uniform streamwise spacing in low aspect ratio pin fin arrays. *Proceedings of the ASME Turbo Expo 2013: Turbine Technical Conference and Exposition* 3A: V03AT12A050. https://doi.org/10.1115/GT2013-95889
107. Metzger DE, Berry RA, Bronson JP (1982) Developing heat transfer in rectangular ducts with staggered arrays of short pin fins. *J Heat Transfer* 104: 700–706. https://doi.org/10.1115/1.3245188
108. VanFossen GJ (1982) Heat-transfer coefficients for staggered arrays of short pin fins. *J Eng Power* 104: 268–274. https://doi.org/10.1115/1.3227275
109. Zhang J, Han HZ, Li ZR, et al. (2021) Effect of pin-fin forms on flow and cooling characteristics of three-layer porous laminate. *Appl Therm Eng* 194: 117084. https://doi.org/10.1016/j.applthermaleng.2021.117084
110. Luo L, Yan H, Du W, et al. (2022) Numerical study of a novel curved pin fin for heat transfer enhancement within aeroengine turbine blade. *Aerosp Sci Technol* 123: 107436. https://doi.org/10.1016/j.ast.2022.107436
111. Zeng L, Deng D, Zhong N, et al. (2021) Thermal and flow performance in microchannel heat sink with open-ring pin fins. *Int J Mech Sci* 200: 106445. https://doi.org/10.1016/j.ijmecsci.2021.106445
112. Ruan Q, Xu L, Xi L, et al. (2023) Cooling performance of droplet-shaped Kagome truss structure combined with jet array impingement composite cooling structure. *Case Stud Therm Eng* 51: 103558. https://doi.org/10.1016/j.csite.2023.103558
113. Almansour AS, Morscher GN (2020) Tensile creep behavior of SiCf/SiC ceramic matrix minicomposites. *J Eur Ceram Soc* 40: 5132–5146. https://doi.org/10.1016/j.jeurceramsoc.2020.07.012
114. Vedula V, Shi J, Liu S, et al. (2006) Sector rig test of a ceramic matrix composite (CMC) combustor liner. *Proc ASME Turbo Expo 2006: Power Land Sea Air* 2: 255–259. https://doi.org/10.1115/GT2006-90341
115. Sun J (2007) Evaluation of ceramic matrix composites by thermal diffusivity imaging. *Int J Appl Ceram Technol* 4: 75–87. https://doi.org/10.1111/J.1744-7402.2007.02121.X
116. Mensch A, Thole KA, Craven BA (2014) Conjugate heat transfer measurements and predictions of a blade endwall with a thermal barrier coating. *J Turbomach* 136: 121003. https://doi.org/10.1115/1.4028233
117. Pu J, Zhang T, Huang X, et al. (2022) Overall thermal performances of double-wall effusion cooling covered by simulated thermal barrier coatings. *J Therm Sci* 31: 224–238. https://doi.org/10.1007/s11630-022-1561-5
118. Huang X, Pu J, Wang JH, et al. (2020) Sensitivity analysis of internal layout and coating thickness to overall cooling performances of laminated cooling configurations with surface thermal barrier coatings. *Appl Therm Eng* 181: 116020. https://doi.org/10.1016/j.applthermaleng.2020.116020
119. Kim KM, Moon H, Park JS, et al. (2014) Optimal design of impinging jets in an impingement/effusion cooling system. *Energy* 66: 839–848. https://doi.org/10.1016/j.energy.2013.12.024

120. Lee KD, Kim KY (2009) Optimization of a cylindrical film cooling hole using surrogate modeling. *Numer Heat Transfer Part A* 55: 362–380. https://doi.org/10.1080/10407780902720858
121. Mostofizadeh AR, Adami M, Shahdad MH (2018) Multi-objective optimization of 3D film cooling configuration with thermal barrier coating in a high pressure vane based on CFD-ANN-GA loop. *J Braz Soc Mech Sci Eng* 40: 211. https://doi.org/10.1007/s40430-018-1145-1
122. Liu R, Li H, You R, et al. (2025) Multi-objective optimization methodology on cooling performance for a novel laminated cooling structure with pin-fins and slot hole. *Appl Therm Eng* 265: 125621. https://doi.org/10.1016/j.applthermaleng.2025.125621
123. Li W, Tan X, Xiao X, et al. (2023) Multiobjective optimization of double-wall cooling structure of integrated strut flame stabilizer and sensitivity analysis of parameters. *J Aerosp Eng* 36: 04023040. https://doi.org/10.1061/JAEEEZ.ASENG-4525
124. Wang Y, Zhu J, Cheng Z, et al. (2024) Intelligent optimization method for real-time decision-making in laminated cooling configurations through reinforcement learning. *Energy* 291: 130434. https://doi.org/10.1016/j.energy.2024.130434
125. Yang L, Min Z, Yue T, et al. (2019) High resolution cooling effectiveness reconstruction of transpiration cooling using convolution modeling method. *Int J Heat Mass Transfer* 133: 1134–1144. https://doi.org/10.1016/j.ijheatmasstransfer.2019.01.010
126. Yang L, Wang Q, Huang K, et al. (2020) Establishment of a long-short-term-memory model to predict film cooling effectiveness under superposition conditions. *Int J Heat Mass Transfer* 160: 120231. https://doi.org/10.1016/j.ijheatmasstransfer.2020.120231
127. Chouchen M, Ouni A, Mkaouer MW, et al. (2020) Recommending peer reviewers in modern code review: a multi-objective search-based approach. *Proceedings of the 2020 Genetic and Evolutionary Computation Conference Companion*, 307–308. https://doi.org/10.1145/3377929.3390057
128. Newman MEJ (2005) Power laws, Pareto distributions and Zipf's law. *Contemp Physic* 46: 323–351. https://doi.org/10.1080/00107510500052444
129. Narukawa K (2013) Effect of dominance balance in many-objective optimization. In: Purshouse, R.C., Fleming, P.J., Fonseca, C.M., Greco, S., Shaw, J. (eds) Evolutionary Multi-Criterion Optimization. EMO 2013. *Lecture Notes Comput Sci* 7811: 276–290. https://doi.org/10.1007/978-3-642-37140-0_23
130. Balaji V, Narendranath S (2023) MOGA and TOPSIS-based multi-objective optimization of wire EDM process parameters for $Ni_{50.3}$-$Ti_{29.7}$-Hf_{20} alloy. *CIRP J Manuf Sci Technol* 47: 158–167. https://doi.org/10.1016/j.cirpj.2023.09.005
131. Liu X, Zhao J, Yu Y, et al. (2024) BIM-based multi-objective optimization of clash resolution: A NSGA-II approach. *J Build Eng* 89: 109228. https://doi.org/10.1016/j.jobe.2024.109228
132. Iweh CD, Akupan ER (2023) Control and optimization of a hybrid solar PV-Hydro power system for off-grid applications using particle swarm optimization (PSO) and differential evolution (DE). *Energy Rep* 10: 4253–4270. https://doi.org/10.1016/j.egyr.2023.10.080
133. Konak A, Coit DW, Smith AE (2006) Multi-objective optimization using genetic algorithms: A tutorial. *Reliab Eng Syst Saf* 91: 992–1007. https://doi.org/10.1016/j.ress.2005.11.018
134. Wang C, Zhang JZ, Wang C, et al. (2020) Multi-optimization of a specific laminated cooling structure for overall cooling effectiveness and pressure drop. *Numer Heat Transfer Part A* 79: 195–221. https://doi.org/10.1080/10407782.2020.1835105

135. Ismayilov F, Akturk A, Peles Y (2021) Systematic micro heat sink optimization based on hydrofoil shape pin fins. *Case Stud Therm Eng* 26: 101028. https://doi.org/10.1016/j.csite.2021.101028
136. Deb K, Agrawal S, Pratap A, et al. (2002) A fast and elitist multiobjective genetic algorithm: NSGA-II. *IEEE Trans Evol Comput* 6: 182–197. https://doi.org/10.1109/4235.996017
137. Moon MA, Kim KY (2014) Analysis and optimization of fan-shaped pin-fin in a rectangular cooling channel. *Int J Heat Mass Transfer* 72: 148–162. https://doi.org/10.1016/j.ijheatmasstransfer.2013.12.085
138. Li P, Kim KY (2008) Multiobjective optimization of staggered elliptical pin-fin arrays. *Numer Heat Transfer Part A* 53: 418–431. https://doi.org/10.1080/10407780701632759
139. Nguyen NP, Maghsoudi E, Roberts SN, et al. (2023) Shape optimization of pin fin array in a cooling channel using genetic algorithm and machine learning. *Int J Heat Mass Transfer* 202: 123769. https://doi.org/10.1016/j.ijheatmasstransfer.2022.123769
140. Bahman Jahromi H, Kowsary F (2024) A comprehensive parametric study and multi-objective optimization of turbulent jet array impingement for uniform cooling of gas turbine blades with minimized compression power. *Int J Therm Sci* 201: 109035. https://doi.org/10.1016/j.ijthermalsci.2024.109035
141. Kusterer K, Tekin N, Bohn D, et al. (2012) Experimental and numerical investigations of the nekomimi film cooling technology. *Proceedings of the ASME Turbo Expo 2012: Turbine Technical Conference and Exposition* 4: 1299–1310. https://doi.org/10.1115/GT2012-68400
142. Kusterer K, Bohn D, Sugimoto T, et al. (2007) Influence of blowing ratio on the double-jet ejection of cooling air. *Proc ASME Turbo Expo 2007: Power Land Sea Air* 4: 305–315. https://doi.org/10.1115/GT2007-27301

AIMS Press